Biosynthesis of Titanium Oxide Nanoparticles Using Root Extract of *Kniphofia Foliosa* and its Application for Dye Sensitized Solar Cell

By: Eneyew Tilahun

A Thesis Submitted to the Department of Applied Chemistry

School of Applied Natural Science

In Partial Fulfillment of the Requirements for the Degree of

Master of Science in Chemistry (Physical Chemistry)

Office of Graduate Studies

Adama Science and Technology University

August, 2018

Adama, Ethiopia

Biosynthesis of Titanium Oxide Nanoparticles Using Root Extract of *Kniphofia Foliosa* and its Application for Dye Sensitized Solar Cell

By: Eneyew Tilahun

Advisor: Fedlu Kedir (PhD)

Co - advisor: Bedasa Abdisa (PhD)

A Thesis Submitted to the Department of Applied

Chemistry

School of Applied Natural Science

In Partial Fulfillment of the Requirements for the Degree of

Master of Science in Chemistry (Physical Chemistry)

Office of Graduate Studies

Adama Science and Technology University

August, 2018

Adama, Ethiopia

Approval Sheet

Submitted by

Name	Signature	Date

As a thesis research advisors, We hereby certify that we have read and evaluated this thesis prepared under our guidance by Eneyew Tilahun. We recommended the paper to be submitted as fulfilling the requirements for the Degree of Master of Science in Chemistry (Physical Chemistry).

Advisor	Signature	Date
Co-advisor	Signature	Date

We, the undersigned, members of the boards of examiners of the final open defence by Eneyew Tilahun, we have read and evaluated his thesis entitled "Biosynthesis of Titanium Oxide Nanoparticles Using Root Extract of *Kniphofia foliosa* and its Application for Dye Sensitized Solar Cell" and examined the candidate. This is, therefore, to certify his thesis work and has been accepted in partial fulfillment of the requirments of the degree of Master of Science in Chemistry (Physical Chemistry). Complies with the regulation of the University.

Internal Examiner	Signature	Date
External Examiner	Signature	Date
Chair person	Signature	Date
Department Head	Signature	Date
School Dean	Signature	Date

DECLARATION

I hereby declare that the thesis entitled "Biosynthesis of Titanium Oxide Nanoparticles Using Root Extract of *Kniphofia foliosa* and its Application for Dye Sensitized Solar Cell" has been carried out by me under the supervision of Dr. Fedlu Kedir and Dr. Bedasa Abdisa, during the year 2017/2018 as part of Master of Science Program in Physical Chemistry. I further declare that this work has not been submitted to any other Universities or institutions for the award of any degree. All quotations and their sources are specifically acknowledged by means of references.

Name : Eneyew Tilahun

Signature _____

This M.Sc thesis has been submitted for examination with our approval as thesis advisors.

Advisor Name: Fedlu Kedir (PhD) Co-advisor Name: Bedasa Abdisa (PhD)

Signature _____ Signature _____

Date of Submission _____

DEDICATION

This M.Sc thesis is dedicated to my beloved families, especially to my Father Tilahun Bekele and to my Mother Zewditu Leyekun, whose advice, support, prayers and love helped me all along the right way and made me who I am today. They will always be in my heart forever!.

AUTHOR'S BIOGRAPHY

The author was born in May 1990 G.C at Mankusa, Jabitehnan Woreda, West Gojam Zone, Amhara National Regional State. He attended his elementary school at Mankusa elementary School and secondary school at Mankusa Secondary School. He attend his preparatory school at Finoteselam Damot Perparatory School. After completion of preparatory school, he joined Adama Science and Technology University in 2014 G.C and graduated with BSc degree in Chemistry in July 7, 2016. Soon after graduation, the author was got a sponsership from Adama Science and Technology University in 2017/2018 and joined school of graduate studies in the same year to pursue his M.Sc study in the field of Physical Chemistry.

ACKNOWLEDGEMENTS

First and foremost I would like to thank the only almighty God, the embodiment of wisdom who provides health, strength and accurate insight into reality for his divine intervention during my research work.

Although this thesis work ultimately represents my accomplishments, I have benefited significantly from multiple peoples that I would like to acknowledge. First and foremost, I am grateful to goes to my hard working advisors: Dr. Fedlu Kedir and Dr. Bedasa Abdisa for their excellent supervision and scientific input in this research work. It is a great privilege and honor for me to be advised by them. I owe special thanks to my mentor, Dr. Fedlu Kedir, whose unique scientific passion and extensive knowledge I strongly admire and will always aspire to achieve; his patience, daily guidance and support have kept me on the right track all the way to the end. His positive influence will always be a guide as I venture out on my own to tackle challenging scientific problems. I am lucky to be guided and advised by him and in general his friendly approach makes me a successful man.

Then I would like to express my genuine heartfelt gratitude to my co-advisor, Dr. Bedasa Abdisa for his invaluable suggestion, comments, corrections, professional & technical guidance throughout my work for the successful accomplishment of this thesis.

I greatly acknowledge Dr. Osman Ahmed from School of Material Sciences and Engineering for his assistance in interpreting XRD and SEM spectrum. I never forgot his great contribution in facilitating conditions for me to send samples to Taiwan National University in order to characterize using SEM-EDS, UV-Vis and TEM and in general for all friendly discussions I have made with him from the starting up to the end of this work. Again I would like to give the dearest and greatest thanks to Dr. Milkyas Endale and Mr. Kebede Shenkute, from School of Applied Natural Science, department of Applied Chemistry program for their willingness to share their knowledge and experience about the plant *kniphofia foliosa* and *kniphofia schemperi* that were used for the biosynthesis of titanium oxide nanoparticles and for the extraction of natural sensitizer, respectively.

I would like to express my sincere gratitude to all academic, technical and support staff of the Program of Applied Chemistry, Adama Science and Technology University, for providing the necessary knowlledge, assistance and facilities to conduct my research work. Finally I would like to thank greatly Adama Science and Technology University for giving me the opportunity to join this postgraduate program and for free sponsorship of my study.

TABLE OF CONTENT

Contents **Page**

LIST OF ABBREVIATIONS AND ACRONYMS

CE Counter electrode

CNT Carbon nanotubes

CO_2 Carbon dioxide

CV Crystal violet

D Average crystalline diameter

DI Dionized water

DSSC Dye sensitized solar cell

DTA Differencial thermal analyzer

E_g Band gap energy

EQE External quantum efficiency

FF Fill factor

FTIR Fourier transformation infrared spectroscopy

FTO Fluorine doped tin oxide

HOMO Highest occupied molecular orbital

IPCE Incident photon to current conversion efficiency

ITO Indium doped tin oxide

I-V Current-voltage

J_{SC} Short circuit current

K Scherre's constant

KS *Kniphofia schemperi*

LHE Light harvesting efficiency

LUMO Lowest unoccupied molecular orbital

MOS Metallic oxide semicondactore

NPs Naoparticles

OSC Organic solar cell

PEC Photoelectrochemical cell

PEDOT Poly(3,4-ethylenedioxythiophene)

PEG Polyethyl glycol

P_{max} Maximum power point

PSC Perovsikte solar cell

PSS Polysrene sulfonate

PV Photovoltaics

PVP Polyvinyl Pyrrolidone

SEM Scanning electron microscope

θ Diffraction angle

TCO Transparent conductive oxide

TGA Thermal gravimetric analysis

TiO_2 Titanum dioxide

UV-Vis Ultraviolet Spectrophotometer spectroscopy

V_{oc} Open circuit voltage

XRD X- ray diffraction

β Full width at half maximum intensity

λ_{max} Wavelength at maximum absorption

LIST OF FIGURES

LIST OF TABLES

LIST OF INDEXS

ABSTRACT

Currently synthesis of nanoparticles (NPs) using plant extracts has attracted a great attention due to its low cost, non-toxicity and environment-friendly nature. In this study pure titanium dioxide NPs were synthesized by biological methods using 0.4 M titanium tetra butoxide as a precursor with the presence of ethanolic root extract of kniphofia foliosa in different ratio and the biosynthesized NPs were tested for their application in dye sensitized solar cells (DSSCs). The biosynthesized NPs were characterized by thermogravimetric analysis (TGA-DTA), X-ray diffraction (XRD), scanning electron microscopy-energy dispersive x-ray spectroscopy (SEM-EDS), transmission electron microscopy (TEM), ultraviolet visible spectroscopy (UV-Vis) and fourier transformer infrared spectroscopy (FTIR). TGA was performed to study the thermal stability of pure TiO_2 NPs and the NPs were stable above 500℃. The crystal structure of the NPs were followed by XRD analysis and the analysis revealed that the biosynthesized NPs have particle size in the range of 8.17 - 10.15 nm. SEM analysis indicated that the biosynthesized NPs posses spherical in shape. The EDS analysis revealed the presence of only Ti and O in the prepared nano samples confirming the purity of the biosynthesized NPs. TEM analysis shows the internal structure of the nanoparticles as spherical. The UV-Vis investigation confirmes the formation of titanium oxide NPs, the absorbance peak was exist in between 298 nm - 314 nm. FTIR study confirmed the presence of amines,carboxylic acids, phenols, alcohols, protiens, enzymes. The pastes of biosynthesized NPs were used as photoanodes in DSSCs (a device used for converting absorbed light in to electricity). In this study natural sensitizer was extracted from roots of kniphofia schemperi using absolute ethanol (99.9%) as a solvent and in addition to this, 0.001 M crystal violet dye was prepared. At the end, devices were fabricated using k.schemperi and crystal violet and TiO_2 (1:1, 2:1 and 1:2) photoelectrodes which showed the power conversion efficiency of 0.117%, 1.3% and 0.039%, respectively. IPCE analysis of the biosynthesized TiO_2 (2:1, 1:2 and 1:1) photoelectrode shows 18.01%, 6.64% and 2.66%, respectively.

Keywords:- Titanium dioxide (TiO_2), biosynthesis, *kniphofia foliosa*, DSSCs, sensitizers.

1. INTRODUCTION

1.1. Background of the Study

Energy consumption is one of the most important aspects in people's everyday life. It exists in different forms, from burning woods to obtain fire in prehistoric times to electricity productions in modern age. However due to the rapid growth in industrialization in many countries the original sources of energy that people used to harvest have shown signs of deficiency. Therefore, people started searching for new resources for energy production. At the same time, people also realized the damages that the energy production has done to the environment. One of the challenges faced by this world, is the increase in energy demand following growth of world economy and populations size (Gra¨tzel *et al*., 2012). Therefore, researches have been increased rapidly to seek for clean and renewable energy resources that will power the future.

A search for a clean and sustainable source of energy free of carbon has therefore become an important issue for scientists and researchers. The primary supply of sustainable and ecofriendly energy is one of the major challenges of the twenty first century. Recent advances in solar energy conversion technologies based on organic semiconductors as light harvesting layer, such as dye-sensitized solar cells and organic solar cells, employ metallic oxide semiconductor (MOS) nanostructures for efficient charge extraction and transportation between the electrodes and organic molecules (Grätzel *et al.*, 2012).

Increasing concerns about energy crisis, climate change, decreasing availability of fossil fuels and environmental issues are motivating the research on sustainable and renewable energy resources. The key for the success of this goal lays in the development of efficient energy conversion and storage devices. Increasing global energy and environmental challenges demand clean and sustainable energy sources to support the activities of modern society. One of the most feasible technologies is to convert solar energy directly into electricity by solar cells. Among sustainable technologies, such as tidal power, solar thermal, hydropower and biomass, photovoltaic technology is regarded as the most efficient onces (Gong *et al.*, 2012). Solar cells or Photovoltaics, also known as the process of converting sunlight into electricity directly, was first discovered in 1839 by Becquerel, a French physicist and Nobel Laureate upon observing light dependency voltage between electrodes in an electrolyte. Dye sensitized solar cells (DSSCs) invented by Michael Grätzel since 1991 became a very popular alternative energy sources to silicon based solar cells because of their great potential to convert solar energy into electrical energy at low cost. In the field of photovoltaic research, dye sensitized solar cells (DSSCs) have attracted considerable attention with strong absorption of visible light since it was first developed by Michael

Gr*ä*tzel. As long as the PV cells are exposed to sunlight, the cell can produces an electric current proportional to the amount of light it receives. PV cells can help to reduce the widespread dependence on dwindling oil reserves and mitigate adverse effects on the environment.

Solar cells based on dye sensitized porous nanocrystalline TiO_2 photoanode with attractive performance was first reported by (O´Regan *et al.*, 1991). A dye sensitized solar cell (DSSC) is a low cost solar cell belonging to the group of thin film solar cells, whch is based on a semiconductor formed between a photo sensitized anode, an electrolyte, and a photo electrochemical systems. Dye-sensitized solar cells (DSSCs) are a third generation photovoltaic special cells that efficiently and effectively converts visible light into electrical energy. Invented in 1991 by Michael Gr*ä*tzel and *Ó*regan, and it is given the name because it mimics the photosynthesis process by absorbing natural sun light.

The transition MOSs such as TiO_2 are well known for their ability to exchange charges with condensed molecules, making them a viable and cost effective candidate to be used in the photovoltaic devices. In dye sensitized, MOSs serve as a scaffold, in photovotaics such as DSSCs and perovskite solar cells, and as a charge transport layer in organic and DSSCs. The function of scaffold in DSSCs is to facilitate charge separation and charge transport, whereas that of the transport layers is to conduct one type of charge carrier while blocking the other type (Jose *et al.*, 2009).

It was stated that dye sensitized solar cell (DSSC) established on the mechanism of novel regenerative photoelectrochemical processes with an efficiency of 7.9%. Following theis success, extensive research has been carried out in this field to increase the power conversion efficiency (PCE) of DSSCs by incorporating n-type metallic semiconductors such as TiO_2, ZnO, Nb_2O_5, $SrTiO_3$, and SnO_2 and their composites as photoanode materials (O´Regan *et al.*, 1991).

The interconnected TiO_2 nanoparticles in DSSCs is widely used as the mesoporous electrode film layer, because it is beneficial for adsorption of large amount of dye molecules due to its large surface areas. However, the overall performance of DSSCs can be limited by the electron transport in the nanocrystal boundaries of TiO_2 nanoparticles and the electron recombination with the electrolyte during the electron migration process. To avoid this problem, many researchers have reported that one dimensional TiO_2 nanostructures can be used as replacements of three dimension nanoparticles to facilitate electron transfer. In addition to their unique electron properties, one dimensional TiO_2 nanostructures also function as a light scattering materials for DSSCs (Kang *et al.*, 2008).

There are several reasons why we choose and focus on DSSCs instead of other energy sources is that the conversion of solar energy in to electrical energy possesses some advantages over other sources of energy. First, solar energy does not create greenhouse gases as it generates electricity (Emery, 2015). A greenhouse gas can absorb radiation in the infrared range which is the fundamental cause of the greenhouse effect, the main reason leading to global warming right now. Second, solar energy is easily available all around the world. Unlike wind power and hydro energy, solar energy spread out more evenly in the world; thus, the geographical location of a country is not likely to prevent the countries from taking advantage of solar energy. The world solar energy potential clearly indicates that most part of the world could potentially utilize the solar energy as the primary energy resources, especially for countries near the equator. The solar energy is essentially inexhaustible because it is radiation from the sun and there is a large quantity of solar radiation accepted on the earth every day. Third, there is a minimum byproduct compared to other energies during their formation, no disposal method necessary. Forth, less space is required and relatively low cost and high efficiency (Hagfeldt and Gr*ä*tzel., 1995). Fifth, conversion from sunlight to electricity is direct, so that bulky mechanical generator systems are unnecessary. Photovoltaic arrays can be installed quickly and in any size required or allowed. Sixth, the environmental impact is minimal, requiring no water for system cooling and generating no byproducts. Seventh, good performance in diverse light conditions: high angle of incidence, low intensity, partial shadowing. Eight, low cost: inexpensive to manufacture, roll to roll processing possible. Finally, it is light weight and flexible.

1.2. Statement of the Problem

In recent years the most common methods to obtain energy are based on fossil fules and many other non renewable sources. But these common methods to obtained energy are associated with high level of CO_2 emissions. As a result of these CO_2 emissions in to the natural environment which causes global warming, it is necessary to develop alternative methods to generate green energy (Dye sensitized solar cell) using green synthesized nanoparticles (Realpe *et al.*, 2015).

During the last decades different researches were done on DSSCs using inorganic complex dyes and commercially available and chemically synthesized titanium oxide nanoparticles and the corresponding performance of the fabricated DSSCs was also measured (Liao *et al.*, 2011). But the use of this commercially available and chemically synthesized titanium oxide nanoparticles is not cost effective and at the same time it is not environmentally friendly. Eventhough different researchs were done on the synthesis of nanoparticles for dye sensitized solar cell (DSSCs) applications, still now synthesis of

nanoparticles by green methods using indigenous plant extracts for DSSCs applications is not a wide spread area and if we successfully convert the solar energy into electricity our need of renewable energy will be completely satisfied. Still now, according to the knowledge of different researchers, green synthesis of TiO_2 nanoparticles using *kniphofia foliosa* root extracts for DSSC application is not done. Therefore, to the best of my knowledge, the planned research was biosynthesis of TiO_2 nanoparticles using titanium tetra butoxide as a precursors and indigenous medicinal plant, (*Kniphofia foliosa*) root ethanolic extract as a reducing and capping agent which are cost effective and easily availabe and then using the biosynthesized TiO_2 nanoparticles to fabricate DSSCs. Here TiO_2 NPs was used as one component of DSSCs (Photoanode).

1.3. Objectives of the Study

1.3.1. General objective

The general objective of this study was biosynthesis of TiO_2 nanoparticles using *k.foliosa* root extract and fabrication of DSSCs using *k.schemperi* and crystal violet sensitizers and then characterization.

1.3.2. Specific objectives

The specific objectives of this study were:-

- ✓ To biosynthesize TiO_2 nanoparticles using ethanolic root extract of *k.foliosa* and $C_{16}H_{36}O_4Ti$
- ✓ To characterize the biosynthesized TiO_2 nanoparticles using TGA, XRD, SEM-EDS, TEM, UV-Vis and FTIR.
- ✓ To extract natural sensitizer from the roots of *kniphofia schemperi* for photo-sensitization in DSSCs.
- ✓ To fabricate DSSCs using biosynthesized TiO_2 NPs, sensitizers and PEDOT as counter electrode.
- ✓ To characterize the fabricated DSSCs using I-V and IPCE.
- ✓ To evaluate the photovoltaic properties of synthsized TiO_2 NPs in DSSCs using *Kniphofia schemperi* and crystal violet as sensitizers.
- ✓ To test the effect of precursor components ration on photovoltaic parameters.

1.4. Significance of the Study

This study area provides important informations about the biosynthesis method of TiO_2 using *k.foliosa* ethanolic root extracts. The area also provides important informations about the extraction method of natural sensitizer. This study area also gives information about DSSCs performance TiO_2 based

nanostructured materials and a natural sensitizer extracted from indigenous plant roots, *k.schemperi* and a synthetic crystal violet dye. This study can also opens up a door for further explorations on many of Ethiopian indigenous plants for photovoltaic applications.

1.5. Scope of the Study

Biosynthesis of TiO_2 NPs using *k.foliosa* root extract as a reducing and capping agent and then characterization of the biosynthesized nanoparticles using TGA, XRD, SEM-EDS, TEM, UV-Vis, and FTIR techniques. The biosynthesized TiO_2 NPs were used in DSSCs for photovoltaic applications only. Characterization of the fabricated DSSCs was done using J-V and IPCE techniques.

2. LITERATURE REVIEW

2.1. Nanoparticles

New technologies often create new challenges to science in addition to their benefits, raise concerns about health and various environmental problems. Nanotechnology is becoming a new area of increasing research and industrial interest since the 1980. Nanotechnology is dealing with the production of materials in a nanometer scale level, normally from 1 to 100 nm. The development of nanotechnology has resulted in a growing public debate on the toxicity and environmental impact of direct and indirect exposures to nanoparticles (NPs). The word "nano" is originated from a Greek word whose meaning is extremely small or dwarf particles. Nanoparticles are cluster of atoms having at least one dimension in the size range of 1 - 100 nm (Brayner., 2008).

Nano structured materials have attracted the attention of researchers because of their variety of anticipated features in the technology. Owing to their unique optical, magnetic, catalytic, and electrical properties, nanoparticles have potential applications in various fields. The physicochemical properties of NPs are different as compared to those of their bulk counterparts owing to the fact that surface area to volume ratio increases as the size decreases. Various semiconductor oxide nanoparticles play an important role in various applications such as self-cleaning, gas sensors, optics, Photoelectrochemical devices, solar cell applications, photocatalysis, cosmetic industry, antimicrobial activity and medicinal applications (Mandal *et al.*, 2006).

2.2. Biosynthesis of TiO_2 Nanoparticles

Ever since inception of life on the earth, the biological entities and inorganic materials have been in constant touch with each other. Due to this regular interaction, life could sustain on this planet with a well organized deposit of minerals. Recently the global research focus is aimed towards the interaction between inorganic molecules and biological species. The development of reliable experimental protocols for the synthesis of nanoparticles over a range of chemical compositions, sizes, and high monodispersity is one of the challenging issues in the current nanotechnology. The synthesis of TiO_2 nanoparticles with specific morphologies and properties is one of the most important aspects of nano science which studies materials whose size lies within the nanometer range (10^{-9} m). The synthesis and assembly of titanium nanoparticles would benefit from the development of clean, nontoxic and environmentally acceptable green chemistry procedures, probably involving organisms ranging from bacteria to fungi and green plants. But the microbial mediated synthesis of nanoparticles requires maintenance of organisms and optimum parameters such as temperature, pH and other factors for microbial growth. In order to develop

the simple green synthesis, the plant extract mediated process is considered as a suitable method for the synthesis of titanium oxide nanoparticles (Mandal *et al.*, 2006).

Our environment is suffering huge damage by the release of large amount of hazardous chemicals, gases or toxic substances into the environment due to rapid industrialization and urbanization. Therefore, there is an urgent to learn about the use of natural products for development of advanced functional nanomaterials (Vijaylaxmee *et al.*, 2014). Traditionally most of the metal and metal oxide nanoparticles were routinely synthesized by various methods. During the last few decades, several approaches such as hydrotherma, solvothermal, sol-gel, direct oxidation, chemical vapor deposition, electro-deposition, sonochemical, chemical bath deposition, and microwave methods are used for the synthesis of TiO_2 nanostructures (Rodriguez-Sanchez *et al.*, 2000). But these methods are very costy, toxic, demanding high pressure, unease of separation and potentially hazardous. Hence, there is an increased demand to develop a high yielding, low cost, non toxic and mono-disperse nanoparticles leads to exploit biological and eco-friendly methods to synthesize TiO_2 nanoparticles.

Now a day, a new and innovative approach was attempted for biosynthesis of TiO_2 nanoparticles which are rapid, cost effective, and environmentally benign in the context to green nanotechnology and may be directly used in agricultural, biomedical and engineering sectors. Recent process via green chemistry route (green synthesis) involoves the use of environment friendly materials such as plant extracts (leave, flower, bark, root, seed, and peels), bacteria, fungi and enzymes in the synthesis of titanium dioxide nanoparticles (Tamasa and jiha., 2013). Green synthesis provides more advantages over physical methods and chemical methods because it is very cost effective, easy process and scalable for large scale production. This method doesn't requires high temperatures, high pressure, costy equipment and hazardous chemicals. Moreover, plant based nanoparticle synthesis approaches are easy to scale up and are traditionally also favoured because of their environment friendliness.

Due to the diversity of plants, nanoparticles synthesis from plant extract has known an interesting subject across the world as different plant species are being rapidly investigated and used in nanoparticles synthesis. An eco-friendly method for the green synthesis of TiO_2 NPS using ethanolic extract of neem as biotemplate was developed and found that the synthesized TiO_2 NP was anatase crystal form (Shilpa *et al.*, 2012). In the previous time different researchers synthetized TiO_2 nanoparticle from leaves of *nyctanthes arbor-tristis* in 2011. The finest powder that was obtained by grinding and sieving dried leaves was mixed with ethanol in order to extract ethanolic leaf extracts. Titanium tetraisoproxide was used as a precursor for TiO_2 nanoparticles synthesis from ethanolic leaf

extracts of *nyctanthes arbor-tristis*. The obtained TiO_2 nanoparticles were spherical in shape and their sizes were ranging from 100 nm to 150 nm.

TiO_2 NPs was produced by the reaction between *latex of jatropha curcas* leavs and $TiO(OH)_2$. XRD and TEM revealed that the size of synthesized TiO_2 NPs were 100 - 200 nm. FTIR spectra of latex capped TiO_2 NPs showed the presence of capping/ stabilizing agents like protein/ peptide material which also prevent the nanoparticles from agglomeration (Hudlikar *et al.*, 2012).

TiO_2 NPs was biosynthesized using aqueous extracts of *eclipta prostrate* leave as biotemplating agent. The precursor that has been used was of $TiO(OH)_2$. The obtained TiO_2 NPs were spherical in shape and their size ranged from 36 nm to 68 nm. And the calculated average size of synthesized TiO_2 NPS was 49.5 nm (Rajakumar *et al.*, 2012).

TiO_2 NPs was also synthesized using *rice straw* powder as biotemplate with titanium tetra isopropoxide aqueous solution and acetic acid. The above mentioned solution was heated at 80℃ to form gel. The obtained gel was dried at 80℃ and calcined at 500℃ for 5 hours. The average crystalline size of synthesized TiO_2 NPs was from 10 - 20 nm (Ramimo *et al.*, 2014).

TiO_2 NPs was formed using aqueous extract of *psidium guajava* leaf and $TiO(OH)_2$ used as precursor. To synthesize TiO_2 NPS 20 ml aqueous extract of *p.guajava* was added into 80 ml of $TiO(OH)_2$ at room temperature under stirred condition for 24 hours. The XRD pattern of the synthesized TiO_2 NPs showed the presence of both anatase (110) and rutile(111) crystallographic structure. The calculated average size of plant mediated synthesized TiO_2 NPs was found to be 32.58 nm (Kumar *et al.*, 2014).

Plant extracts may act both as reducing and stabilizing agents in the synthesis of TiO_2 nanoparticles. The use of different parts of plants in the biosynthesis of TiO_2 nanoparticles and their applications, holds immense potentials towards the environment. The source of the plant extract is known to influence the characteristics of the nanoparticles. This is because different extracts contain different concentrations and types of organic reducing agents (Baker *et al.*, 2013).

Various parts of green plants such as leaves, stems, roots and seeds can be used for synthesis of TiO_2 and other metal nanoparticles. It has been reported that, the primary and secondary metabolites present with in the different parts of plants are well known as natural resources that are responsible for the green synthesis of different nanoparticles which is used as reducing agent (Hoffmann *et al.*, 1995). The green synthesized TiO_2 NPs shows the best photocatalyst activity due to its long thermodynamic stability and strong oxidizing power (Baker *et al.*, 2013).

In general, the green process involves three important steps, (1) solvent medium selection, (2) environmental benign reducing agent selection and (3) selection of non-toxic capping agent in nanomaterials synthesis. Researchers reported that the rate of synthesis of nanoparticles is very high when they use plant extracts instead of microorganisms for biosynthesis of metal nanoparticles, which is a more rapid and reproducible process. The nature of plant extract affects the kind of nanoparticles synthesized in a highly critical manner with the source of plant extract being the most vital factor affecting the morphology of synthesized nanoparticles. Interestingly, this is so because different plant extracts contain different concentrations of biochemical reducing agents (Shilpa *et al.*, 2012).

2.3. Applications of Titanium Dioxide (TiO_2) Nanoparticles

Titanium dioxide is known as titanium (IV) oxide or titania, with the chemical formula of TiO_2. Compared with its bulk counter part, TiO_2 nanomaterials have been passionately studied over the past decades due to their potential applications in many areas. TiO_2 is very useful because of its non-toxicity, chemical stability when exposed to acidic and basic compounds, low cost, its highly oxidizing power, wide band gap, good mechanical resistance and high optical transmittance in visible and IR spectral range, chemical sensor, electronics, optics, optoelectronics, transparent, power circuits and many other advantages. Nanocrystalline TiO_2 semiconductors are well known for various applications such as photovoltaics, photocatalytics, photonic crystals, photochromics and it also find applications in biomedical sciences such as bone, tissue engineering and in pharmaceutical industries due to its non-toxicity nature. Recently, photovoltaic applications using TiO_2 for dye sensitized solar cells has become the focus of considerable research efforts. Titania is the most important photocatalyst having the potential applications in purification and treatment of water and air, regarding to environmental protection. For photocatalytic applications, titanium dioxides can be either used in the form of powders or coatings. It has been determined that the energy conversion efficiencies of the photovoltaic devices that benefit nanocrystalline TiO_2 are critically dependent on the size of the particles (Carp *et al.*, 2004 and Loo *et al.*, 2012).

2.4. The Chemistry of Red Hot poker (*Kniphofia Foliosa*)

Kniphofia are herbaceous perennials growing from rhizomes. Most of the species of *Kniphofia* are ever green while a few are deciduous and sprout again in the early summer. The genus *Kniphofi*a named after the German botanist Johann Hieronymus *Kniphof* belongs to the subfamily of Asphodeloideae (Dahlgren *et al.,* 1985). Due to their tall scarlet or red flowers the genus is commonly known as ‘red hot pokers’. The genus *Kniphofia* (sub-family Asphodeloideae, family Asphodelaceae) comprises 70 species

mainly confined to Africa with the center of diversity being South Africa. Fifteen *Kniphofia* species have been recorded in Eastern Africa, of which seven occur in Ethiopia, among of these seven specious, five of them including *Kniphofia foliosa*, *Kniphofia hildebrandtii*, *Kniphofia isoetifolia*, *Kniphofia insignis* and *Kniphofia schimperi* are endemic (White., 2002). *K. foliosa* is a perennial herb which grows on road sides, over grazed areas with scattered trees and is commonly distributed in the mountainous regions of central and northern Ethiopia. The specific name 'foliosa' refers to the many crowded rosulate leaves at the base. Traditionally the roots of *K. foliosa* have been used for the treatment of different ailments including menstrual pains, infertility, abdominal cramps, wounds, malaria, chest complaint, gonorrhea and hepatitis. The plant also used to remove endoparasites in cattle. Previous phytochemical investigations of this plant have resulted in the isolation of monomeric anthraquinones, phenylanthraquinones and dimeric anthraquinones. The plant is known to elaborate monomeric, dimeric anthraquinones and phenylanthraquinones, some of which exhibit diverse biological activities. Some of the chemical compounds extracted from the roots of *k. foliosa* are indicated in Figure 1 as 3, 5, 8-trihydroxy-2-methylnaphthalen-1; 4-dione, one monomeric anthraquinone; chrysophanol and knipholone anthrone respectively (Abate *et al.*, 1989 and Dagne *et al.*, 1984).

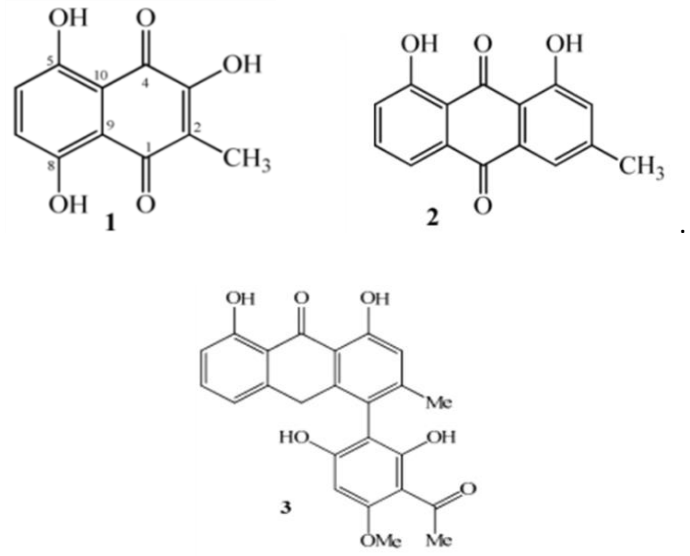

Figure 1. Isolated compounds extracted from roots of *k. foliosa* (Dagne *et al.*, 1984).

Since the roots of *k. foliosa* metabolite materials serve as excellent reducing agents which includes phenolic compounds, alkaloids, sterols and as a result, in addition to its traditional medicinal usage for household remedy against various human ailments, roots of *k. foliosa* extracts could also be used for the biosynthesis of nanoparticles in order to exclude the addition of external stabilizing agents during synthesis process because of the presence of various functional groups within the roots of the plant extracts.

2.5. Basic Principles and Components of DSSCs

Basically DSSCs contains several components such as transparent anode made up of a glass sheet treated with a transparent conductive oxide layer; a mesoporous oxide layer (typically, TiO_2) deposited on the anode to activate electronic conduction; a monolayer charge transfer dye covalently bonded to the surface of the mesoporous oxide layer to enhance light absorption; an electrolyte containing redox mediator in an organic solvent effecting dye regenerating; and a cathode made of a glass sheet coated with a catalyst (typically, platinum) to facilitate electron collection. In DSSCs, the basic photovoltaic principle relies on the visible photo-excitation of dye molecules. Upon light irradiation, the monolayer of the sensitizer is photoexcited; the excited electrons are injected into the conduction band in the TiO_2; the electrons penetrate through the nanocrystalline TiO_2 film to the back contact of the conducting substrate, and flow through an external circuit to the CEs; at the CEs, the oxidized component of redox couple in the electrolyte is reduced; the oxidized form of the sensitizer is finally regenerated by the reduced component of redox couple in the electrolyte (Jose *et al.*, 2009). In this overall process, there are two major recombination loss processes that limit the total conversion efficiency within the DSSCs: the photoinjected electrons in TiO_2 can recombine directly with the oxidized dye molecules or with the oxidized form of the redox couple in the electrolyte as indicate in the diagram at number 7. The general principles of DSSCs is shown in Figure 2. Overall, the device generates electric power from light without suffering any permanent chemical transformation.

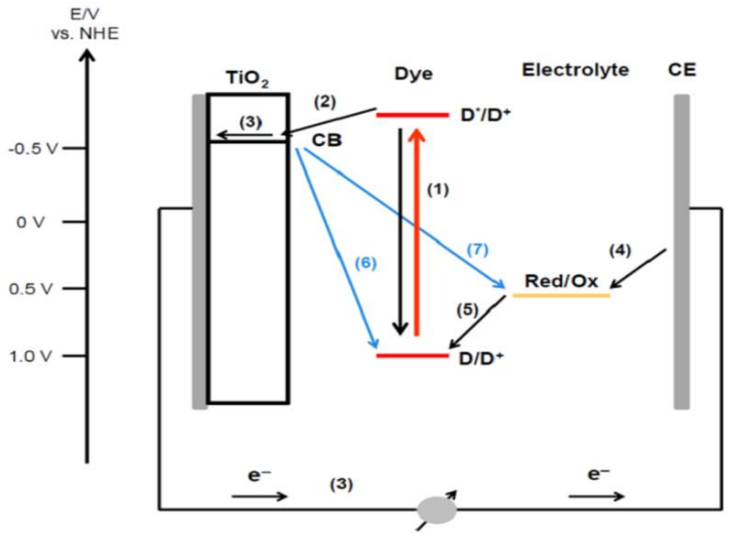

Figure 2. Principles of DSSCs (Grätzel., 2004).

2.5.1.Titanium dioxide nanoparticles in DSSCs

The need for DSSCs to absorb far more of the incident light was the driving force for the development of mesoscopic semiconductor materials with an enormous internal surface area. The major break through in DSSCs was the use of a high surface area nanoporous TiO_2 layer. A single monolayer of the dye on the semiconductor surface was sufficient to absorb essentially all the incident light in a reasonable thickness (several μm) of the semiconductor film. TiO_2 became the semiconductor of choice with advantage properties of cheap, abundant, and non toxic (Vlachopoulos., 1988).

The standard DSSC technology is based on a liquid electrolyte and glass substrate which are made of a transparent conducting glass electrode coated with porous nanocrystalline TiO_2. The semiconductor, typically a metal oxide, is responsible for providing the surface for dye adsorption, for collecting electrons from the excited dye and for conducting them towards the external circuit. Stable oxides cannot absorb visible light because they have relatively wide band gaps. To be able to absorb light, metal oxide semiconductor materials (e.g TiO_2, ZnO and SnO_2) are sensitized with photosensitizers that are able to absorb visible light (Mbonyiryivuze *et al.*, 2015).

Among all these semiconductors, nanoporous anatase TiO_2 has been chosen as the standard semiconductor in the DSSCs for its excellent performance because it has no photo-degradation phenomena upon excitation compared with other semiconductors which have similar band gap. The higher conduction band edge of anatase leads to higher fermi level and higher V_{OC} in DSSCs application. This large band gap is needed in dye-sensitized solar cell for the transparency of the semiconductor electrode for the wide range of the solar spectrum. A great number of common wide energy band gap semiconductors have been reviewed but anatase TiO_2 is still the most well known and used once. Till now, TiO_2 is the cornerstone semiconductor for dye sensitized nanostructured electrodes for DSSCs. This is due to the fact that the semiconductor is non toxic, easily available and low cost characteristics, TiO_2 has been the mostly preferred semiconductor for photoelectrode (Fan-Tai *et al.*, 2017).

2.5.2. Transparent conductive substrates (TCO)

Conductive substrates must be highly transparent to allow the passage of maximum sunlight to the active area of the DSSCs in order to excite electrons of the dye of the DSSCs. Typically, DSSCs are constructed with two sheets of transparent conductive materials as current collectors for the deposition of the semiconductor and the catalyst. The transparent conductive oxide materials characteristics

determines the efficiency of DSSCs due to the efficient charge transfer of electrical conductivity to minimize energy loss. They are thin layer films that function as a current collector and a support of the semiconductor layer in DSSCs. They have two basic important features: the high optical transparency which allows natural sunlight to pass through to the beneath of the active material without unwanted absorption of the solar spectrum, and the low electrical resistivity which facilitates electron transfer process and reduces energy loss. Typically both FTO and ITO are widely used as conductive substrates in DSSCs (Gong *et al.*, 2012).

Researchers were conducted a study based on FTO and ITO glass substrates sintered at 450ºC. They found that upon sintering, the sheet resistance of ITO increased from 18 Ω cm^{-2} to 52 Ω cm^{-2} while the sheet resistance of FTO remained constant. The overall conversion efficiencies of DSSCs based on FTO and ITO were approximately 9.4% and 2.4%, respectively. Thus, FTO is strongly recommended for use in the fabrication of DSSCs due to its conduction properties and stable sheet resistance temperature. In general TCO should posses the demanding processing conditions for the device preparation without change of its physical properties. The resistance of TCOs will increase, if heated to high temperatures for a long time. However, the TCO typically remains stable up to temperatures slightly above the sintering temperature of nanostructured semiconductors (Huang *et al.,* 2012 and Jasim., 2011).

2.5.3. Counter electrode

To complete the regenerative cycle in a DSSCs, the oxidized form of the redox couple has to be reduced at the counter electrode by the flow of electrons through the external circuit. The task of the counter electrode is to reduce the oxidized species of the redox couple i.e counter electrodes serves to transfer electrons from external circuit to triiodide and iodine in the redox electrolyte. This should be done with as low resistance as possible in order to attain an efficient DSSCs. The most common counter electrode material used for the iodide/triiodide redox system has been thermally deposited platinum nanoparticles. Currently, a layer of platinum coated on transparent conducting oxide (TCO) substrate is widely used as counter electrode in DSSCs. However this is not an economic way for an efficient DSSCs production. Rather different types of carbonaceous materials and conducting polymers such as poly (3,4-ethylenedioxythiophene) (PEDOT) are quite attractive to replace platinum due to their high electronic conductivity, corrosion resistance, high reactivity for triiodide reduction and low cost (Taras *et al.*, 1989).

For metal substrate such as stainless steel, the best efficiency of which is 5.3% has been achieved with Pt as catalyst, which is relatively poor compared to glass substrate based DSSCs. Furthermore, the

DSSC fabricated using stainless based counter electrode with thermal deposition corroded. TiO_2 exhibits good chemical stability with electrolyte compared to stainless steel. The best conversion efficiency of DSSC obtained with TiO_2 based counter electrode is 7.7%. However, to reach lower cost fabrication of DSSC, alternative materials have been investigated such as conducting polymers. Conducting polymers such as PEDOT deposited using electropolymerization is one of the best alternatives in counter electrode synthesis. The best efficiency for these polymers on plastic substrates is about 4.4%. For metal based substrate, with TiO_2 as counter electrode with PEDOT as catalyst, 6.3% efficiency has been reached. Stainless steel based counter electrode also work well with carbon by applied composite film made of carbon aerogel and poly (tetrafluoroethyelene) and in such case it gives an efficiencies as high as 9.2% (Miettunen *et al.*, 2009).

2.5.4. Redox couple electrolytes

A redox couple is the key component in a photoelectrochemical cells, assuming the tasks for dye regeneration and charge transport between the two electrodes, playing a crucial role in determining the photovoltaic performance of DSSCs. An "ideal" redox couple should essentially fulfill a certain requirements as follows: The redox potential of a redox couple should be less negative than the oxidized level of a dye molecule (it should be as positive as possible to maximize the photovoltage), mean while maintaining a sufficient driving force for dye regenerations; Slow electron recombination kinetics at the interface; Negligible visible light absorption; Fast electron transfer kinetics at CEs; Good diffusion properties to avoid mass-transport limitations particularly under higher levels of irradiation; Non-corrosiveness towards collecting metals, and good photochemical stability (Wang *et al.*, 2005).

Iodide/triiodide (I^-/I_3^-) has been used as a redox couple from the very beginning of DSSCs research and has proven to be one of the most versatile redox couples so far combining high overall conversion efficiency of up to 11- 12% and, at the same time, good long-term stability. Due to the corrosive nature and complex redox chemistry of I^-/I_3^- system, a great deal of efforts has been devoted to identifying alternative redox couples to replace the I^-/I_3^- system. The use of iodine free alternative redox couples and their photovoltaic performances in DSSCs have been thoroughly reviewed recently (Shi *et al.*, 2008 and Hamann *et al.*, 2011).

It was reported that, following the invention of low cost dye-sensitized solar cells (DSSCs), redox-couple solid electrolytes have attracted considerable attention in recent years. These electrolytes can eliminate the short coming of the liquid/gel electrolytes, such as leakage/evaporation of organic solvent especially at elevated temperatures, electrode corrosion, a need of hermetic sealing, and scale up of the

manufacturing process. Some characteristics of these electrolytes are: Not absorbing light in the visible region; A high electrical conductivity and low viscosity for faster diffusion of electrons; Good interfacial contact with the nanocrystalline semiconductor and the counter electrode and not desorption of the dye from the oxidized surface and the degradation of the dye (Kusama and Arakawa., 2005).

One disadvantage of liquid electrolyte is that it may limit device stability because the liquid may evaporate when the cell is imperfectly sealed. Currently quasi-solid electrolytes becomes the most alternative once. Quasi-solid electrolytes show better long term stability than liquid electrolytes do and have the merits of liquid electrolytes including high ionic conductivity and excellent interfacial contact property and does not cause desorption and degradation of the dye from oxide surface. These unique characteristics of quasi-solid state electrolytes have been actively developed as highly conductive electrolyte materials for DSSCs, lithuim secondary batteries and for fuel cells. Quasi-solid state electrolytes are usually prepared by incorporating a large amount of a liquid electrolyte into organic monomer or polymer matrix, forming a stable gel with a network structure (Murphy., 1998).

2.5.5. Sensitizers in dye sensitized solar cell

The reason why a dye-sensitized solar cell is dye sensitized is because the band gap of the semiconductor used is so wide that it only absorbs light in the UV region. The function of the sensitizer is to absorb the incident light, inject the excited electron into the semiconductor, converting the absorbed light in to electrical energy with the aid of a semiconducting photoanode and become regenerated by the redox couple in the electrolyte. Therefore, the cell performance is mainly dependent on the type of dyes used as a sensitizers (Mulati *et al.*, 2012).

Dyes applied in DSSCs are categorized into two types which are organic and inorganic dyes. Inorganic dyes comprises of metal complex, such as polypyridyl complexes of ruthenium and osmium, metal porphyrin, phthalocyanine, inorganic quantum dots and many others, while organic dyes comprises of natural and synthetic dyes. Ruthenium based complexe dyes are considered as good sensitizers for DSSCs because of their intense charge transfer absorption over the entire visible ranges and highly efficient metal to ligand charge transfer. These complex dyes are capable of delivering DSSCs with high conversion efficiency as compared to natural DSSCs (Reza and Ahmad., 2013).

DSSC sensitized with organic dyes have relatively lower power conversion efficiencies than those sensitized with metal complexes. However pure organic dyes have many advantages for their application in DSSC such as lower cost, high absorption coefficient and easy control of redox potential. In order to obtain even cheaper dyes for DSSC, metal free organic dyes are strongly desired. Metal free organic

dyes offer superior molar extinction coefficients, low cost, and a diversity of molecular structures. Researchers were studied various commercially available organic dyes with catechol groups, triphenylmethynedye, anthraquinone dye and xanthene dye as sensitizers for dye sensitized solar cells. The absorption maxima of these dyes ranges from 470 to 570 nm with cut off wavelengths at around 700 nm which makes them potential candidates for light harvesting in dye sensitized solar cells (Mosurkal *et al.*, 2004). All dyes showed quasi reversible wave with oxidation potentials ranging from 0.6 to 0.9 V. The short-circuit photocurrent density (I_{SC}), the open-circuit photovoltage (V_{OC}), the fill factor (FF) and the overall energy efficiency (η) were estimated to be 3 mA/cm^2, 443 mV, 33% and 0.74%, respectively. Similarly crystal violet known as methyl violet is a triaryl methane dye is one of the common organic dye that emitted a brilliant color when exposed to visible light and used in DSSCs (Koumura *et al.*, 2006). The name refers to its color and in ethanol this organic dye exhibits strong absorption at around 440 nm. The chemical structure of crystal violet dye is shown in Figure 3.

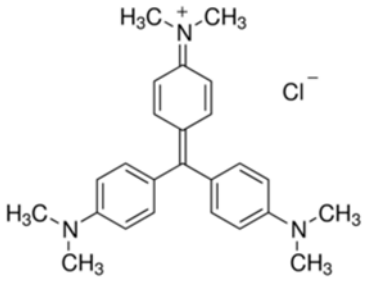

Figure 3. Chemical structure of crystal violet (Koumura., 2006).

In addition to the above different types of dyes used in DSSCs, natural dyes can be used for the same purpose with an acceptable efficiency. Natural dyes have several advantages, like ease of extraction with minimal chemical procedures, large absorption coefficients, low cost, non-toxicity, environmentally friendly, easily biodegradable and wide availability. Thus, several dyes extracted from natural pigments including anthocyanins, carotenoids and chlorophylls have been used as sensitizers in DSSCs. Therefore, the use of natural dyes have been considered as potential candidates to enhance the light response of semiconductors in active layers of solar cells and have been demonstrated in several solar cell materials. Naturally, the fruits, roots, flowers and leaves of plants shows different colors from red to purple and include different natural dyes which can be extracted using simple procedures and used for DSSC fabrication (Wang *et al.*, 2005).

Previously it was reported on home made DSSC prepared using natural dyes extracted from raspberries, shami-berries, grapes, hibiscus and chlorophyll pigment extracted from young green lemon leafs. The open-circuit voltage was found to vary from 0.255 V to o.429 V, the short circuit current density from

0.017 mA/cm^2 to 0.269 mA/cm^2, the fill factor varies from 54.1% to 64.8% and the conversion efficiency various from 0.04 to 1.50. Among these sensitizers, raspberries were reported to have the best photosensitization effect due to the better intraction between the carbonyl and hydroxyl groups of anthocynin molecule present in the raspbery which effectively binds with the surface of TiO_2 porous films (Mounir *et al*, 2012). In the previous years researchers have used various natural dyes extracted from black rice, capsicum, erythrina variegata flower, rosa xanthina, and kelp as sensitizers and found that the dye from black rice showed the best photosensitized effect, which was due to the better interaction between the carbonyl and hydroxyl groups of anthocyanin molecule on black rice extract and the surface of TiO_2 porous film (Hao *et al.*, 2006). Similarly it was also reported on the usage of *ipomoea* fruit and *spinach* extracts as sensitizers for DSSC and resulted in efficiencies of 0.257% and 0.131%, respectively (Chang *et al.*, 2010).

Some characteristics of an efficient photosensitizers are: Possess Highest occupied molecular orbital level more positive than the redox potential of the electrolyte and the lowest unoccupied molecular orbital more negative than the CB of the semiconductor; Broad spectral coverage: intense absorption in the visible region (400 - 900 nm); Adsorb strongly on the surface of the semiconductor; High extinction coefficient; Stable in its oxidized form allowing it to be re-reduced by an electrolyte and stable enough to carry out ~10^8 turnovers (20 years of cell operation); Fast kinetics for injection and regeneration. Natural pigments extracted from fruits, vegetables, flowers and roots, such as chlorophyll, carotenoids, anthocyanins, and betalains have been extensively investigated as sensitizers for DSSCs (Reza and Ahmad, 2013).

Chlorophyll derivatives:- Chlorophyll is the major light-absorbing pigment in green plants, algae and cyanobacteria. Chlorophyll has magnesium as its central metal ion, and the large organic molecule to which it bonds is known as a porphyrin. The porphyrin contains four nitrogen atoms bonded to the magnesium ion in a square planar arrangement as shown in Figure 4. There are two main types of chlorophylls; these are chlorophyll a and chlorophyll b, which are differing only on the side chain composition of R, which are -CH_3 and -CHO and each of the chlorophyls have two absorption peaks around 425 and 662 nm and 463 and 645 nm, respectively. These groups are responsible for absorbance of different wavelength range of light. Both of these two chlorophylls are very effective photoreceptors (Kayama *et al.*, 2009).

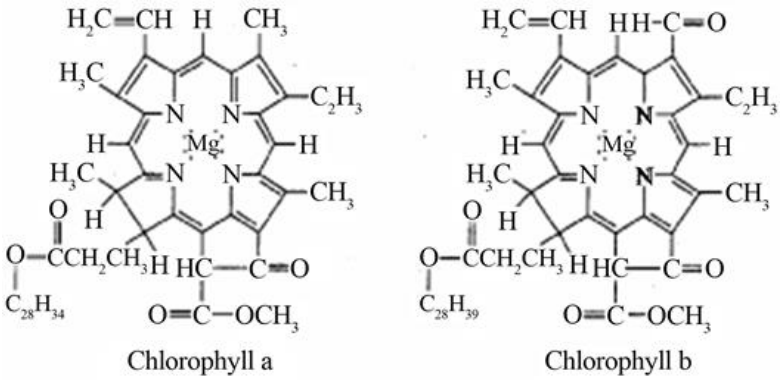

Figure 4. Structure of chlorophyll a and b (Kayama *et al.,* 2009).

Anthocyanins:- Anthocyanin compounds exhibit a wide band in the UV-visible region of the spectrum due to charge transfer transition. The anthocyanins constitute a major flavonoid group that is responsible for cyanic colors ranging from salmon pink through red and violet to dark blue of most flowers, fruits and leaves of angiosperms. Some times they are present in other plant tissues such as roots, tubers and stems. The presence of the carbonyl and hydroxyl functional groups in the structure of anthocyanin helps an excess anchoring of the dye on the surface of TiO_2 film and also causes an easy electron transfer from the anthocyanin molecule to the conduction band of TiO_2. The maximum absorption of anthocyanin extracts ranges from 510 to 548 nm depending on the fruit, leaves and flowers or the solvent used. Figure 5 shows the basic chemical structure of most anthocyanin pigment (Chappel *et al.*, 2005).

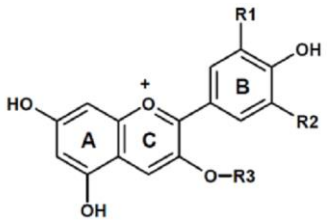

Figure 5. General structure of abundant anthocyanin (Chappel *et al.,* 2005).

Anthocyanin absorbs different parts of the visible and ultraviolet spectrum, depending not only on the type of anthocyanin, but also on the type of sugar attached, where on the carbon skeleton this sugar is attached, pH, complexes formed with metal cations and the presence of colorless flavonoids.

Betalains:- Betalain pigments represent an additional class of organic natural dyes of potential interest. They are water-soluble nitrogen-containing alkaloid pigments that are found in some families of plants belonging to the order caryophyllales and some fungi, but not found in plants containing anthocyanin pigments. They can be divided into betacyanins (generally appear red to red violet in color) and betaxanthins (generally appear yellow in color) based upon their molecular structure and color as well as

wavelength absorbance, which are 535 - 550 nm, 475 - 480 nm ranges, respectively (Hedbor and Klar., 2005). The general structure of both betacyanins and betaxanthins are indicated in Figure 6.

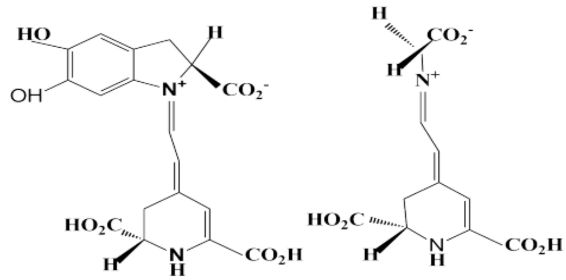

betacyanins betaxanthin

Figure 6. General structure of betalaine: betacyanins and betaxanthins (Hedbor and Klar., 2005).

2.6. Characterization of Dye Sensitized Solar Cells (DSSCs)

2.6.1. Characterization of DSSCs using J -V curve

One of the most essential performance characterization technique of a solar cell is the current-voltage (J-V) measurements. DSSCs constructed using nanomaterials, natural dyes and PEDOT as counter electrode can be characterized with the help of current density voltage (J-V) techniques and it gives different informations about the fabricated DSSCs. From J-V curve the important photovoltaic parameters such as fill factor, short circuit current density, open circuit voltage and power conversion efficiency can be extracted.

Fill Factor (FF):- The fill factor also known as curve factor is a measure of the junction quality and series resistance of the DSSC. It is a the ratio of the maximum power output (I_{MP}) to the product of short circuit photocurrent and open circuit photo voltage, P_{MP}, J_{SC} and V_{OC}.

$$FF = \frac{J_{MP} \times V_{MP}}{J_{SC} \times V_{OC}} \ldots\ldots\ldots\ldots\ldots\ldots\ldots\ldots (1)$$

Power Conversion Efficiency (η):- The power conversion efficiency of a solar cell is defined as the maximum power produced by the cell (P_{max}) divided by the power (intensity) of the incident light on the representative area of the cell. The overall conversion efficiency (η) of the dye sensitized solar cell is determined by the photocurrent density (J_{SC}), the open-circuit potential (V_{OC}), the fill factor (FF) of the cell and the intensity of the incident light (P_{in}).

$$\eta = \frac{P_{MP}}{P_{in}} = \frac{J_{SC} \times V_{OC} \times FF}{P_{in}} \ldots\ldots\ldots\ldots\ldots\ldots\ldots\ldots (2)$$

Where P_{MP} is maximum power output, P_{in} is the power of incident light, V_{OC} is open circuit voltage, J_{SC} is the short circuit current and FF is the fill factor. As it can be seen from equation (2), the only way to improve the power efficiency of DSSC is to increase J_{SC},V_{OC}, or FF.

Short-Circuit Current Density (Jsc):- To remove the dependence of the solar cell area, it is more common to list the short-circuit current density (Jsc in mA/cm^2) rather than the short-circuit current. The short-circuit current density (Jsc) is the photocurrent per unit area (mA/cm^2) when an illuminated cell is short circuited. It is dependent on several factors such as the light intensity, light absorption, injection efficiency and regeneration of the oxidized dyes.

$$J_{SC} = qG(L_n+L_p) \quad \ldots\ldots (3)$$

Where q is the charge, G is the generation rate, L_n and L_p are the electron (e^-) and hole (h^+) diffusion lengths respectively. Equation (3) indicates that J_{SC} depends strongly on generation rate and the diffusion length.

Open Circuit Voltage (V_{OC}):- Open circuit voltage (V_{OC}) is the maximum voltage attainable in a solar energy conversion device. That is the difference in potential between the two terminals in the cell under light illumination when the circuit is open. The theoretical maximum of the cell V_{OC} is determined by the difference between the fermi level of the semiconductor and the redox potential of the hole-conductor (Chang *et al.*, 2010). An equation for V_{OC} is found by setting the net current equal to zero in the solar cell equation to give:

$$V_{OC} = \frac{nkT}{q} \ln(\frac{I_{ph}}{I_o} +1) \quad \ldots\ldots (4)$$

Where, k is the Boltzmann constant, T is the absolute temperature, q is the charge on an electron, n is the ideality factor of the diode (for an ideal diode n = 1), I_o is the inverse saturation current density which is the current density flowing under sufficiently high reverse bias, I_{ph} is the photogenerated minority carrier current (which is opposite in sign to the dark current) and is equal to the product of the absorbed photon flux and the charge on an electron (Hafez *et al.*, 2010).

2.6.2. Characterization of DSSCs using IPCE

Incident photon to current efficiency also called external quantum efficiency, is a measure of how efficient a solar cell is in producing photo-generated charges at a given frequency. IPCE is measured for a specific light wavelength and describes how efficiently the light of a specific wavelength is converted to current, that is (electrons out) /(photons in). It is given by the Equation (5) below.

$$IPCE\% = \frac{1240 \text{ x } J_{SC}}{\lambda_{P_{in}}} \text{ x}100\% \quad \ldots\ldots\ldots\ldots\ldots\ldots\ldots\ldots\ldots\ldots\ldots (5)$$

Where J_{sc} is short circuit current density (mA/cm^2), λ is the excitation wavelength (nm) and P_{in} is the incident photon intensity (W/m^2), 1240/λ refers to the energy of photons in eV (electro volt) (Vahermaa *et al.*, 2010).

3. MATERIALS AND METHODS

Experimental Sites:- Biosynthesis of TiO_2 nanoparticles using ethanolic root extract *of k. foliosa*, extraction of natural sensitizer from roots of *k.schemperi*, characterization of the biosynthesized TiO_2 NPs using DTA/TGA, XRD and preparation of some of the components of DSSCs was done at Adama Science and Technology University. Characterization of the biosynthesized nanomaterials using SEM-EDS, TEM and UV-Vis spectroscopy was done at Taiwan National University. Characterization of the biosynthesized nanoparicles using FTIR spectroscopy, fabrication of most of the components of DSSCs, the assembly and finally characterization of the fabricated DSSCs was done at Addis Ababa University, department of Chemistry.

3.1. Chemicals and Reagents

Different chemicals and reagents as well as solvents were used. Such as distilled water, HCl, titanium tetra butoxide (Acros organics, 98%), acetone (Sigma Aldrich), acetonitrile (Sigma Aldrich), sodium hydroxide (Sigma Aldrich), I_2 (Sigma Aldrich), NaI (BDH), 1-ethyl-3-methyl immidazolium iodide (EMIMM-I: Sigma Aldrich), acidified H_2O, Isopropanol (Riedel-de Haen), Polyvinyl Pyrrolidone (PVP, Sigma Aldrich), $C_2H_5)_4NBF_4$ (Sigma Aldrich), (ethylenedioxythiophene) (EDOT: Sigma Aldrich), absolute ethanol (Lab Tech Chemicals), triton X-100 (Sigma Aldrich), crystal violet (Sigma Aldrich) and conductive FTO glass substrate (Sigma Aldrich).

3.2. Apparatus and Equipments

Different apparatus and instruments were used such as:- thermo gravimetric analysis (TGA/DTA: DTG-60H Shimadzu Co., South Korea), FTIR (Perkin elmer65), XRD (XRD-7000 X-ray diffractometer, Shimadzu Co., South Korea), UV-Vis spectrophotometer (JASCO V-670UV-Vis spectrophotometer equipped with a diffuse reflectance attachment for powder samples), SEM-EDS (FE-SEM, JEOL-JSM 6500F, made in Japan), TEM (HRTEM, Tecnai F20 G2, Philips, Netherlands), digital electronic balance, oven, furnace, electronic centrifuge, ultrasonic bath, glass filters, computer controled electrochemical analyzer (CHI630A), test tube, borsosilicate glass, magnetic stirrer, mortar and pestle, cylindrical glass, pH meter, micro grinding machine, hot plate, micropipets, spatulas, erlenmeyer flask, volumetric flask, different types of beakers, plastic bottles, aluminum foil, towels and many others were used.

3.3. Collection of the Plant Sample for the Biosynthesis of TiO_2

Kniphofia foliosa, also called tritoma, red hot poker, torch lily, knofflers or poker plant, is a genus of perennial flowering plants in the family of Asphodelaceae, first described as a genus in 1794, was collected from Bale Zone, Oromia Regional State after conducting the field surveys. The collected roots were first surface cleaned and washed thoroughly with distilled water several times. Then the cleaned roots were cut in to small pieces and allowed under shadow dry and was weighed. The roots of *k.foliosa* were used to make ethanolic extracts for the next procedures.

3.4. Methods

3.4.1. Extraction of the root (Broth solution)

The roots of *kniphofia foliosa* were thoroughly washed using distilled water to remove the unwanted impurities such as scum, dust and other particulates. After that the root samples were cut into small pieces and were allowed under shadow dry at room temprature. The dried roots of *k. foliosa* were grinded using plant grinding machine and then were packed within a plastic bottle followed by covering the whole body of the plastic bottle with aluminum foil. Extraction of the roots of *k. foliosa* for the biosynthesis of TiO_2 NPs was done by taking 5 gram of powder of *k. foliosa* root by measuring using electronic balance and was placed in to a 500 mL erlenmeyer flask followed by addition of 200 mL of ethanol (absolute ethanol, 99.9%). The erlenmeyer flask containing the two components was placed on to a hot plate with magnetic stirrer. The two components was allowed to boil at 50℃ for about 35 minutes. Then the boiled suspension formed in the solution was allowed to cool for about 45 minutes and was filterd using whatman number one filter paper. The final extract of the solution was collected and stored at 4℃ within a refrigerator for the biosynthesis of TiO_2 nanoparticles within (1:1, 2:1 and 1:2) ratios. The filtrate ethanolic root extract was used as reducing and capping agent for the biosynthesis of TiO_2 nanoparticles from titanium tetra butoxide precursor (Santhosh *et al.*, 2014).

3.4.2. Biosynthesis of TiO_2 NPs

Titanium tetra butoxide is a chemical compound with the formula of $C_{16}H_{36}O_4Ti$ (Acros Organics, 98%), was used as a precursor for the biosynthesis of TiO_2 nanoparticles within different ratio using ethanolic root extract of *k. foliosa*. To biosynthesize TiO_2 NPs, different ratio of the plant (*k.foliosa*) and titanium tetra butoxide were used. To examine the effect of proportion of titanium tetra butoxide and *k.foliosa* ethanolic extract on the size and crystallite of TiO_2 NPs, a 1:1, 2:1 and 1:2 ratios of the

precursor salt and *k. foliosa* root extract were used during the biosynthesis process. Then three different samples were prepared by taking different ratios by volume of precursor salt solution and plant extract.

For **1:1 ratio**: 50 mL of 0.4 M titanium tetra butoxide and 50 mL of *k.foliosa* root extract.

For **2:1 ratio**: 66.7 mL of 0.4 M titanium tetra butoxide and 33.3 mL of *k.foliosa* root extract.

For **1:2 ratio**: 33.3 mL of 0.4 M titanium tetra butoxide and 66.7 mL of *k.foliosa* root extract.

$$Ti\{OCH_2(CH3)_2\}4 + 4C_2H_5OH + \text{plant extract} \rightarrow Ti(OH)_4 + 4(CH_3)_2\text{-}CH_2\text{-O-}C_2H_5 + \text{byproduct}$$

$$Ti(OH)_4 \xrightarrow{\text{stirring}} TiO_2 + 2H_2O$$

For the biosynthesis of TiO_2 nanoparticles within 1:1, 2:1 and 1:2 ratio, approximately (50 : 50), (67.7 : 33.3) and (33.3 : 67.7) mL was taken, respectively and this was done using 0.4 M of titanium tetra butoxide in a separate erlenmeyer flask. In each case the erlenmeyer flask containing the two components was placed on to a plate with magnetic stirrer with out applying of heat. In each of the different ratios, a small sized magnetic stirrer was placed in to the erlenmeyer flask containing the extract and the precursor solution and the resulting solution was allowed to stirred for about 4 and half hours. Then the stirred solution in each case was stayed at room temperature for about 20 minutes and then its pH value was measured using a pH meter and then a small drop of 1 M of sodium hydroxide solution was added for each of the individual ratio as a precipitating agent. After addition of a small drop of sodium hydroxide solution for each of the individual ratio, the resulting solution was stirred for a few minutes to maintain uniform distribution of the added base. Then the formed TiO_2 NPs was allowed to stay within a refrigeretor for over night at the same condition for each of the different ratio. After that, the formed precipitate for each of the individual ratio was washed with absolute ethanol and then appropriate volume of distilled water was added in to the formed precipitate and again placed within a refrigerator for one day. The formed titanium dioxide nanoparticles were acquired by centrifugation at 1000 rpm for about 30 minutes. Then the centrifuged particles were first washed with ethanol (ethanol absolute, 99.9%) and the formed precipitate was separated and after that small amount of distilled water was added and again subjected to centrifugation at 1000 rpm for about 25 minutes. The formed TiO_2 NPs were collected using a crucible ceramic dish and placed in to a drying oven for over night at 100℃.

3.5. Characterization Techniques of Biosynthesized TiO_2 NPs

3.5.1. Characterization of TiO_2 NPs using TGA

Thermal gravimetric analysis (TGA) techniques are widely used to evaluate the thermal degradation behaviour and thermal stability of materials (Ramimoghadam *et al.*, 2013). Thermal gravimetric analysis (TGA) of the biosynthesized NPs was carried out using a simultaneous differential thermal analysis DTA-TGA (DTG-60H, Shimadzu Co., South Korea) apparatus to determine the calcination temperature of the biosynthesized nanoparticles. From the biosynthesized TiO_2 NPs, approximately 5.939 mg of the uncalcinated TiO_2 nanoparticles was taken and placed in a platinum crucible on the pan of the microbalance and heated from room temperature to 900^0C, using aluminium as inert atmosphere and then DTA and TGA data were collected.

3.5.2. Characterization of TiO_2 NPs using XRD

The crystalline structure of the biosynthesized titanium oxide nanoparticles were investigated by the x-ray diffraction using x-ray diffractometer (XRD-7000 x-ray Diffractometer, Shimadzu Co., South Korea). XRD spectrum was recorded from 10^0 to 80^0 with 2θ angles using CuKα (λ = 1.54056 A^0) radiation operated at 40 kV and 30 mA. Debye Scherrer's equation indicated in equation 6, was used to estimate the average crystallite size of the biosynthesized nanoparticles (Xu *et al.*, 2008).

$$D = \frac{0.94\lambda}{\beta\cos\theta} \ldots\ldots\ldots\ldots\ldots\ldots\ldots\ldots\ldots\ldots\ldots\ldots (6)$$

Where D is the crystallite size, λ = 1.54056 A^0, is the X - ray source wavelength, β is the full width at half maximum intensity (FWHM) of a peak in terms of radians, and θ is the peak position.

3.5.3. Characterization of TiO_2 NPs using SEM-EDS

From the biosynthesized nano sample, small amount was taken and characterized by field emission scanning electron microscopy-energy dispersive x-ray spectroscopy (FE-SEM, JEOL-JSM 6500F., made in Japan) and provides different informations about the nanoparticles including surface morphology and shape as well as its chemical composition. SEM was also provides detailed high resolution images of the sample by rastering a focused electron beam across the surface and detecting secondary or back scattered electron signal (Pusit *et al.*, 2009).

3.5.4. Characterization of TiO_2 NPs using TEM

Transmission electron microscopy also sometimes called conventional transmission electron microscopy or CTEM) is a microscopy technique in which a beam of electrons is transmitted through a specimen to form an image of the sample and provides informations about the internal structure of the biosynthesized TiO_2 NPs (Figgemeier *et al.*, 2007). The biosynthesized TiO_2 nanoparticles was analysed by using high-resolution transmission electron microscopy (HRTEM, Tecnai F20 G2, Philips, Netherlands) at an accelerating voltage of 200 kV.

3.5.5. Characterization of TiO_2 NPs using UV-Vis spectroscopy

The UV-Vis absorption spectra of the biosynthesized nanoparticles obtained using roots of *k. foliosa* was confirmed by using UV-Vis spectroscopy (JASCO V-670UV-Vis spectrophotometer equipped with diffuse reflectance for powder samples) between a wavelength scan of 200 - 800 nm. From the synthesized TiO_2 NPs, approximately 10 mg of the sample was taken and characterized by using UV-Vis. This characterization technique gives information about the optical properties of the biosynthesized nanoparticles. This characterization technique was also provides information about band gap energy of the biosynthesized TiO_2 NPs using the formula (equation 7) (Vijayalakshmi and Rajendran., 2012).

$$E_g = \frac{hc}{\lambda} \quad \text{..... (7)}$$

Where E_g is energy band gap, h is planks constant, c is speed of light and λ is the maximum wavelength of the biosynthesized TiO_2 nanoparticles.

3.5.6. Characterization of TiO_2 NPs using FTIR

Fourier transformer infrared (FTIR) spectroscopy of the biosynthesized TiO_2 NPs was characterized and recorded using a FTIR spectrophotometer (Perkin Elmer65) in order to analyze and detect surface functional groups of the biosynthesized TiO_2 nanoparticles at the scanning range of 4000 - 400 cm^{-1} (Gao *et al.*, 2007). Measurements of TiO_2 NPs was performed by putting the powder of the biosynthesized NPs on KBr plate.

3.6. Extraction and Preparation of Sensitizers

Enough amounts of roots of *kniphofia schemperi* were collected around Bale Zone Oromia Regional State after conducting the field surveys. Those collected samples were surface cleaned and washed

repeatedly using distilled water and cut in to small pices and then allowed under shadow dry at room temprature. Then when all the moisture contents of the collected pigment samples were removed, it was grind using plant grinding machine followed by packing with a plastic bottle and then covering the hole body of the bottle with aluminium foil and was placed within a dark place. The extract was done by taking 4 g of roots of *k.schemperi* powder and socked within 100 mL of ethanol (ethanol absolute, 99.9%) in a 250 mL erlenmeyer flask. After soaking the powder samples in to the corresponding solvent, the mixture of the solvent and the powder was placed within a dark place by covering with aluminum foil to avoid or to minimize photooxidation. Then the resulting separate solution were kept and stored for about 24 hs at room temperature until the required pigment solution was extracted within the solvent and the solid materials were allowed to settle down overnight and the clear solution of the dye was formed. The clear solutions formed (to be used for sensitization) was separated from solid materials using glass filters (Macht *et al.*, 2012 and Calogero *et al.*, 2010).

Again in this study crystal violet organic synthetic dye was prepared and used. This was done by taking 0.101995 gram of crystal violet dye within a 250 erlenmeyer flask followed by addition of DH_2O up to the mark of the flask to form $1x10^{-3}$ M of the dye followed by covering the erlenmeyer flask with aluminum foil and placing within a dark area to prevent the effect of light /to prevent exposure of light. At the end the optical absorption spectra of the sensitizer was done using Perkin Elmer UV-Vis spectroscopy.

3.7. DSSCs Fabrication Steps

One of the reason, DSSCs has been attracting considerable attention than other energy sources using environmentally friendly biosynthesized photoanode is, because of their simple fabrication process. The fabrication process of dye-sensitized solar cells involved different types of components in order to accomplish the whole assembly. Such as substrate cleaning, TiO_2 photoanade preparation /deposition, photoanode sensitization, preparation of redox electrolyte, preparation and coating of PEDOT counter electrode (Huang *et al.*, 2012). The preparation steps for each of the components and the whole assemply are shown below.

3.7.1. Preparation of the substrate for deposition

The substrate cleaning is believed to be a key process that influences the final performance of the devices. The conductive fluorine doped tin oxide (FTO) glass substrate which has an area of (2 cm x 2.5 cm) substrate was cleaned using distilled water and organic solvents such as, acetone, isopropanol and

absolute ethanol, sequentially using ultrasonicator for about 20 minutes in each different solvents. FTO conductive glass substrates were thoroughly cleaned repeatedly before deposition of film of TiO_2 NPs was carried out.

3.7.2. Semiconductor oxide material paste preparation and deposition

TiO_2 paste was prepared according to the method developed by (Nazeeruddin*et al.*, 1993). This was done by taking 0.76 g in each of the three ratios from the biosynthesized TiO_2 nano powder and was ground in a porcelain mortar with drop wise addition of 1 mL of distilled H_2O containing 0.56 mL of 1 M HNO_3 to prevent reaggregation of the nanoparticles. After the powder had been dispersed by the high shear forces in the viscous paste, it was diluted by drop wise addition of 1.01 mL of distilled water under continued grinding. Finally 0.025 mL of Triton X-100 also was added as a dispersing agent to ease adhesion of TiO_2 nanoparticles and grinding the mixture for additional 30 minutes until the paste becomes uniformly homogeneous. Then the prepared film was ready for deposition. With the conductive side facing up, apply two parallel strips of scotch tape on the edges of the glass plate which was used to monitor the film thickness and to provide non-coated areas for electrical contact. The prepared paste was deposited near the top edge of the FTO glass between the two pieces of the tape and was coated by "doctor blade" method (i.e sliding a paste of TiO_2 with a glass rod on the substrate and spread the paste across the plate with the support of the adhesive tapes on both sides), this process was continued until the layer became homogenous. The tape was removed carefully without scratching the TiO_2 coating. Figure 7 shows doctor-blade technique of biosynthesized titanium oxide paste preparation procedures.

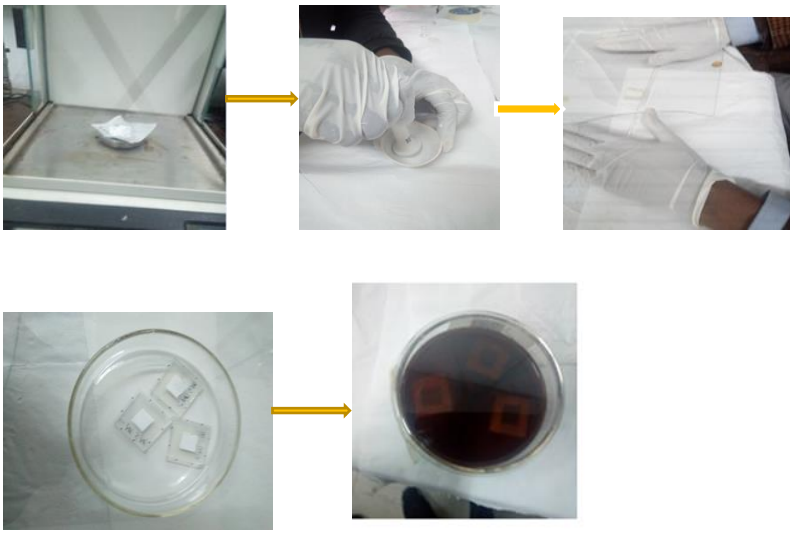

Figure 7. Film preparation procedures using biosynthesized TiO_2.

After drying in air, the as prepared TiO_2 film was sintered at 450°C in a furnace for about 30 minutes to remove the organic solvents which was already used during past prepartion, and this sintering process ensures electrical contact between particles and good adhesion to the FTO conductive glass substrate. After sintered, the formed film was allowed to cool slowly to room temperature.

3.7.3. Electrode sensitization

Sensitizers obtained from roots *of k. schemperi* ethanolic extract and from crystal violet synthetic dyes were adsorbed on top of TiO_2 photoelectrode as follows. The TiO_2 film coated electrode was immersed into the extracted natural dye solution for about 12 hours and for the crystal violet dye the film coated was immersed and stayed for about 6 hs until the monolayer of the TiO_2 film became covered with the dye solution and this sensitization process was performed at room temperature in the dark place for proper adsorption of the dye on the TiO_2 film surface. The dye adsorbed film was taken out and was rinsed with the same solvent used to extract and prepare the sensiyizer (ethanol absolute, 99.9%, distilled water) to remove the unabsorbed dye and any other remain residues available on the surface (Nazeeruddin *et al.,* 1993).

3.7.4. Preparation of redox electrolytes

In this study quasi-solid state electrolyte was used and the preparation is described as follows. The polymer gel electrolyte was prepared according to the method developed by (Fan *et al.,* 2010). This was done by taking 5.3 g of liquid electrolyte which consists of 0.9 M of 1-ethylene-3-methyl immidazolium iodide (EMIM-I) within a 25 mL acetonitrile (high dielectric constant organic solvent) under stirring to form a homogeneous liquid electrolyte. In order to obtain a better conductivity, 0.5 M of sodium iodide was dissolved in the above homogeneous liquid electrolytes and then 0.12 M iodine (I_2) and 35% (w/w) of polyvinylpyrolidone (0.34 g of PVP) was added. Then the resulting mixture was heated at 70 ^{0}C - 80^{0}C under vigorous stirring to dissolve the added PVP polymer followed by cooling down to room temperature to form a gel electrolyte.

3.7.5. Coating counter electrodes

The counter electrode was formed by electrochemical polymerization of 3, 4- ethylenedioxy-thiophene (EDOT) in a three electrode system with one compartment electrochemical cell by using an electrochemical analyzer. The electrochemical cell consists of a pre-cleaned FTO conductive glass which was used as the working electrode, a platinum foil was used as the counter electrode, and a quasi-Ag/AgCl was used as the reference electrode. Then these three electrodes were immersed into a solution

of EDOT and tetra ethyl ammonium tetra flouroborate ($(C_2H_5)_4NBF_4$) in acetonitrile solution. The solution/electrolyte used for the polymerization was obtained by mixing 0.1 M EDOT and 0.1 M ($(C_2H_5)_4NBF_4$) in acetonitrile solvent. The monomer was used as received. The polymerization was carried out potentiostatically at +1.8 V for about 2 second (using bulk electrolysis with coulometry technique). At this potential, the electrode surface was covered with a blue-doped PEDOT film. Then the formed film was rinsed with acetonitrile and dried in air to be used. This electrode is known to be a potential alternative to platinum due to its good conductivity, remarkable stability and a comparatively lower price than Platinum. It also improves the charge transfer between the FTO and the I^-/ I_3^- redox couple (Chang, 2015).

After complete preparation of the whole components, the final step was assembly of the as-prepared DSSCs. The dye covered TiO_2 photoanode and the PEDOT-coated FTO glass counter electrode was assembled as a sandwich type cell by using a drop of the quasi-solid state electrolyte solution deposited in the form of thin film at the surface of TiO_2 films. The assembly of DSSC was completed by attaching the non-titanium dioxide covered area of the photoelectrode and the non-overlapping edge of the counter electrode to the measuring equipment by means of cords and crocodile clips. The photoelectrochemical cell (PEC) was then mounted in a sample holder inside a metal box with an area of 1 cm^2 opening to allow light from the source to enter (Takele *et al.*, 2014). Finally the device was ready for characterization.

3.7.6. Characterization of the fabricated DSSCs

Then the assempled devices are ready for characterization. The photoelectrochemical measurements of the cell were performed using a computer controlled electrochemical analyzer (CHI630A). A 250-W xenon lamp regulated by an oriel power supply (Model 68830) was used to illuminate the PEC. A grating monochromator (Model 77250) placed into the light path and was used to select a wavelength between 300 and 800 nm within a 20 minute interval. The intensity of the incident light was 100 m Wcm^{-2}. The PEC solar cell was then mounted in a sample holder inside a metal box with an area of 1 cm^2 opening to allow light from the source. All the experiments were carried out at ambient temperature.

4. RESULTS AND DISCUSSION

In this section, we mainly presented the result of biosynthesized titanium oxide nanoparticles in different ratios from titanium tetra butoxide as a precursor and roots of *kniphofia foliosa* ethanolic extract as a reducing and capping agent, the different characterization methods of the biosynthesized TiO_2 NPs and its application for dye sensitized solar cell (DSSCs). This chapter also describes the photovoltaic performance of the fabricated DSSCs interms of short circuit current density (J_{SC}), open circuit voltage (V_{OC}), maximum power point (P_{max}), fill factor (FF), power conversion efficiency (η) and incident photon to current conversion efficiency (IPCE) are presented.

4.1.TGA Analysis

Thermal stability of the biosynthesized NPs was determined using TGA/DTA apparatus. Thermo gravimetric and differential thermal analysis was made as a function of temperature. TGA curve shows weight loss from the biosynthesized sample whereas DTA curve indicates the energy gain or loss during the process. The analysis was observed from 25℃ to 900℃ as shown in Figure 8. Below 100℃ the weight loss was observed due to the removal of physically and chemically entrapped water molecules (evaporation of water molecules) from the biosynthesized sample.

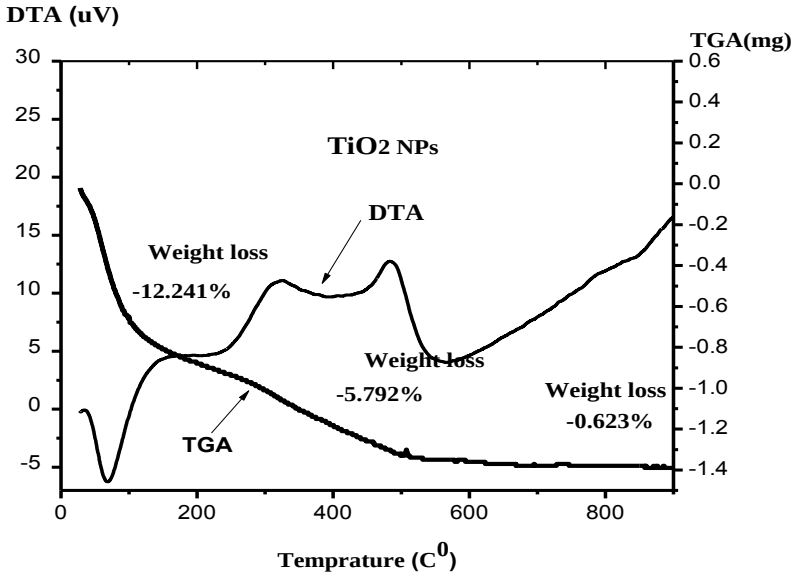

Figure 8. Thermal analysis result for the uncalcinated biosynthesized TiO_2 NPs.

In between the temperature range of 100 - 350 degree celsius, the weight loss was also occurred due to the evaporation of inorganic materials (Muneer *et al.*, 2012). In the DTA curve a small exothermic region around 300℃ indicates the crystallization of TiO_2 sample followed by the oxidation process.

Then the weight loss was again continued up to 483.11℃ associated with a strong exothermic peak in the DTA curve, is due to the decomposition of unreacted organic materials from the sample and the complete removal of the sheath of biomass present over the surface of the sample as well as the condensation of the formed anatase TiO_2 sample. Similar results related to this study were also reported by (Ramimoghadam *et al.*, 2013). TGA/DTA transition shows a weight loss of 5.792% up to 483.11℃ and no considerable weight loss was observed after this temperature up to 900℃. Beyond the temperature of 483.11 degree celsius, no considerable weight loss was observed and the synthesized sample was thermally stable.

4.2. XRD Analysis

Figure 9 (a, b and c) shows the XRD patterns of TiO_2 NPs biosynthesized from titanium tetra butoxide precursor and ethanolic root extract of *k. foliosa* within a 1:2, 1:1 and 2:1 ratios, respectively. As shown in Figure 9 (b), the formation of titanium dioxide nanoparticles was analyzed by x-ray diffraction. The diffraction peaks were in a good agreement with the one which was reported with JCPDS card number of 21-1272. The peaks observed in the samples at 2θ values of ≈ 25.2880, 37.9969, 47.9442, 53.1669, 54.8862, 62.7084, 70.1612, 75.0294 and were along with miller indices values of (101), (004), (200), (105), (211), (204), (220) and (215), respectively. Again as shown from Figure 9 (c), for TiO_2 (2:1) NPs the peaks were observed at 25.3163, 37.9504, 48.0042, 53.9865, 55.0061, 62.6785, 69.9813 and 75.2098 which corresponding miller index values of (101), (004), (200), (105), (211), (204), (220) and (215), respectively. Those results reveals that the biosynthesized NPs have possessed good crystallinity in nature and also diffraction peaks related to impurities were not observed in the XRD pattern, confirming the high purity of the biosynthesized nanomaterials. As the width of the peak increases, size of the particle decreases, which resembles that the present biosynthesized material is within the size of nano range (Pusit *et al.*, 2009). The average crystalline size of the biosynthesized TiO_2 NPs within 1:1 and 2:1 ratio were found to be 8.17 nm and 8.47 nm, respectively which was obtained by using Debye-Schereer's equation, $D = \frac{k\lambda}{\beta\cos\theta}$. Earlier it has been reported that TiO_2 nanoparticles were synthesized using *citrus paradise* peel extract had the dominant 2θ value at 25.3264 anatase form of 101 crystalline structures confirmed by XRD analysis (Chanathaworn *et al.*, 2012). (Nithya *et al.*, 2013) were biosynthesized TiO_2 NPs using aqueous extract of *aloe vera* gel as biotemplate and the XRD pattern of synthesized TiO_2 NPs showed that the crystal structure was predominantly anatase and the calculated average particle size was estimated as 11 nm. Again (Rao *et al.*, 2015) synthesized TiO_2 NPs using aqueous extract of *orange pill* as reducing agent and titanium (IV) isopropoxide as a precursor. From the XRD data, the average crystallite size of the synthesized TiO_2 NPS was calculated as 19 nm.

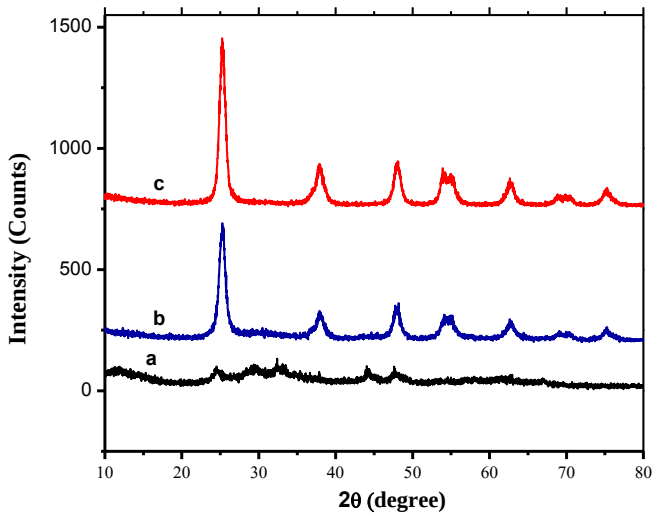

Figure 9. XRD Spectra of biosynthesized TiO_2 NPs within a (1:2), b (1:1) and c (2:1).

As compared to TiO_2 nanoparticles biosynthesized within a 2:1 ratio, XRD data result showed that the average crystallite size of TiO_2 nanoparticles biosynthesized within 1:1 ratio has relatively smaller particle size (8.17 nm) as compared to the average crystalline size of a 2:1 ratio (8.47 nm). This difference may be due to the fact that the greater amount of *k. foliosa* root extract used during the synthesis process results in a more capping agents that intern effectively stabilize the biosynthesized TiO_2 (1:1) nanoparticles. TiO_2 NPs was also biosynthesized within a 1:2 ratio. The peaks were observed at 2θ values of ≈ 25.3109, 37.9020, 47.9424, 55.0861 and 62.0936 along with their miller index values of (101), (004), (200), (211) and (213), respectively. The average crystalline size was found to be 10.15 nm. As it can be observed from the XRD spectra Figure 9 (a), the biosynthesized nano sample loss its crystalline nature due to the fact that the root extract of the added *k. foliosa* used was in excesses which is beyond the coating surface of TiO_2 nanoparticles that in turn results in the formation of agglomeration. A comparison of these results was earlier reported that the XRD analysis of biosynthesized TiO_2 NPs using *catharanthus roseus* leaf extract showed low crystalline nature. Since the biological molecules entered in to the metal oxide matrix is in excess which in turn results in the formation of aggregated nanoparticles (Velayutham *et al.*, 2012). Therefore we can conclude that when the plant extract used islarger than the precursor used, the crystalline nature of the biosynthesized nanoparticles is loss because the extract used is above the coating surface area of TiO_2 nanoparticles already available.

4.3. SEM-EDS Analysis

Morphology of the nanostructured materials is an important characteristic as the performance depends on the morphology. The surface morphology of the biosynthesized TiO_2 nanoparticles obtained was viewed through the high resolution field emission scanning electron microscopy. Figure 10 (a, b and c) shows the SEM images of the biosynthesized nanoparticles within 1:1, 2:1 and 1:2 ratios, respectively. The SEM image reveals the surface morphology of TiO_2 nanoparticles and the particles were found to be spherical in shape with distinct edges. The image also elucidates the increase of particles size with the increase of root of *k.foliosa* ethanolic extract. Moreover, the uniformity of the particles for a (1:1 and 2:1) implies the well association of biomolecules obtained from the root extracts with that of TiO_2 nanoparticles during the biosynthesis process and the presence of the root extact coats the surface of the TiO_2 nanoparticles thus preventing their aggregation.

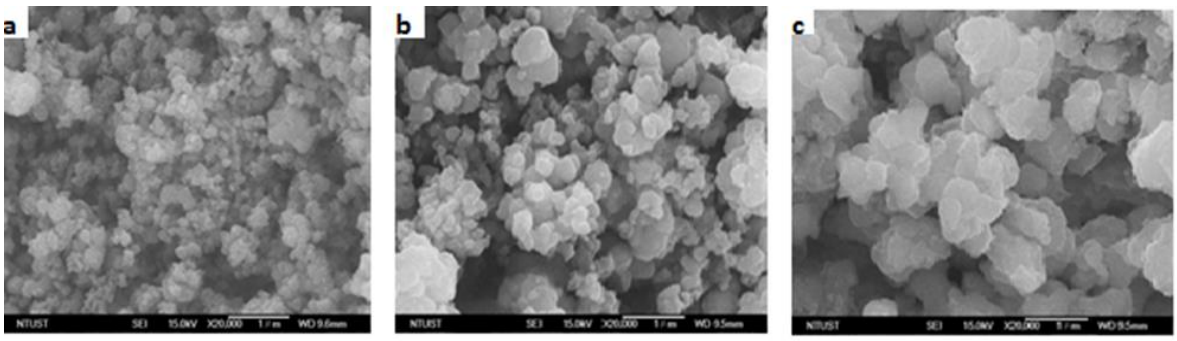

Figure 10. SEM images of TiO_2 Nanoparticles for (a) 1:1, (b) 2:1 and (c) 1:2 ratio, respectively.

The surface morphology of the biosynthesized titanium oxide NPs (a and b) was found to be homogenous in some specific regions. It was reported that, plant phytochemical functionalized nanoparticles are disaggregated and stable with good dispersibility (Archana *et al*., 2012). Which supports the present findings. We could therefore speculate that the phytochemicals present in the roots of *k.foliosa* extract coats the surface of the TiO_2 nanoparticles and thus preventing their aggregation. Privously TiO_2 NPs was biosynthesized using aqueous extract of *c.giganta* flower and the SEM image of the obtained TiO_2 NPs showed that, the formed nanoparticles was aggregated, spherical in shape with average size between 160 - 220 nm (Marimuthu *et al*., 2013). The SEM images of the present study also agreed with XRD results already obtained, i.e. the crystal size in XRD with big size have also big shapes in SEM images. This indicates that TiO_2 NPs have successfully biosynthesized from titanium tetra butoxide in the presence of ethanolic root extract of *k.foliosa* as a reducing nad capping agent within a different ratio and the result was within a nano size range.

Figure 10 (c) the shows the SEM image of TiO_2 (1:2) NPs and the particles shows agglomeration that results in the presence of excess amount of ethanolic root extract of *k.foliosa* which is beyond the coating surface of the TiO_2 nanoparticles already available (Al-Alwani *et al.*, 2015). In addition to this, the result of the SEM image confirms the increase of particles size with the increase of *k. foliosa* root extracts. Moreover, the uniformity of the particles in some regions implies the well association of biomolecules with TiO_2 nanoparticles during the synthesis process. The SEM image shows that the biosynthesized nanoparticles were densely dispersed with a narrow range of dispersion. In addition to this, SEM image reveals that the surface morphology of TiO_2 nanoparticles is spherical in shape with distinct edges and again the result proves that the synthesized nano particles are crystalline in nature and indeed metallic TiO_2 NPs which agrees with that of the XRD results. In all cases the SEM image analysis of the biosynthesized TiO_2 nanoparticles were run within a magnification of 1μm.

To gain a further insight about the biosynthesized TiO_2 nanoparticles in different ratios, the analysis of the sample was performed using EDS techniques. The energy dispersive x-ray analysis of TiO_2 nanoparticles biosynthesized using titanium tetra butoxide at different mixing ratios are shown at Figure 11, index 1 and index 2. It is necessary to verify the presence of desired elements in the biosynthesized nano samples. The absence of any other elements/foreign materials other than titanium and oxygen within the biosynthesized nano sample indicates the elimination of water molecules, ethanol molecules and other organic residues obtained from roots of *k. foliosa* extract during the drying and the calcination process. This also confirms the complete conversion of the starting material, titanium tetra butoxide precursor in to pure TiO_2 nanoparticles. As it can be shown from index 1 of TiO_2 (1:1), the spectrum only reveals the element Ti and O and absence of any foreign materials in the biosynthesized nanoparticles confirms the high purity and absence of any contaminates during the biosynthesis and characterization process.

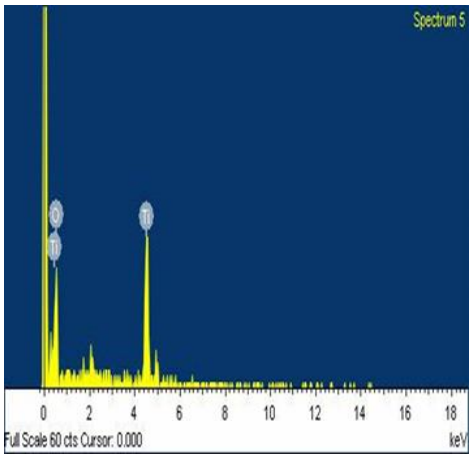

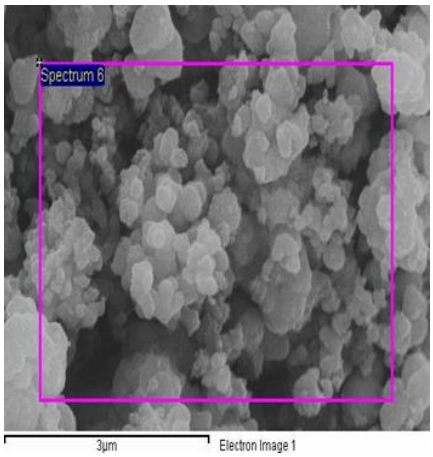

Table 1: Shows quantitative analysis of TiO_2 NPs (2:1)

Element	Wt%	At%
Ok	50.07	75.01
Tik	49.93	24.99
Total	100.00	

Figure 11. SEM images of selected area for EDX spectrum analysis of the biosynthesized TiO_2 (2:1).

The elemental composition of the biosynthesized TiO_2 nanoparticles formed within a 1:2 ratio was also determined by energy dispersive x-ray spectroscopy (EDS) using scanning electron microscopy. It is evident from index 2, the x-ray patterns of the biosynthesized nano sample in which Ti and O are found in the respective EDS spectrum and in addition to this there are no foreign materials present in the spectrum which confirms the purity of the nano sample (Malarkodi *et al.*, 2013).

4.4.Transmission Electron Microscopy (TEM) Analysis

In order to ascertain and gain further informations about the biosynthesized TiO_2 nanoparticles such as internal morphology/structure and crystallinity nature as well as shape, TEM analysis was carried out. The analysis was carried by using high-resolution transmission electron microscopy (HRTEM, Tecnai F20 G2, Philips, Netherlands) at an accelerating voltage of 200 kV. The TEM image exhibit that it was clear that the morphology of the biosynthesized titanium oxide nanoparticles obtained using ethanolic root extract of *k. foliosa* posses spherical/sphere-like structure in shape with smooth surfaces and without any agglomeration as it can be shown from Figure 12. The TEM image showed that the biosynthesized samples were composed of some isolated particles. The TEM image also reveals that, the biosynthesized anatase TiO_2 nanoparticles were found to have good crystalline nature, as it was also supported by the XRD anaylysis results. Previously TiO_2 NPS was produced by the reaction between *latex of jatropha curcas* leaf and $TiO(OH)_2$ precursor & the TEM image revealed that the size of biosynthesized TiO_2 NPs were in between 100 - 200 nm Hudlikar *et al*, (2012).

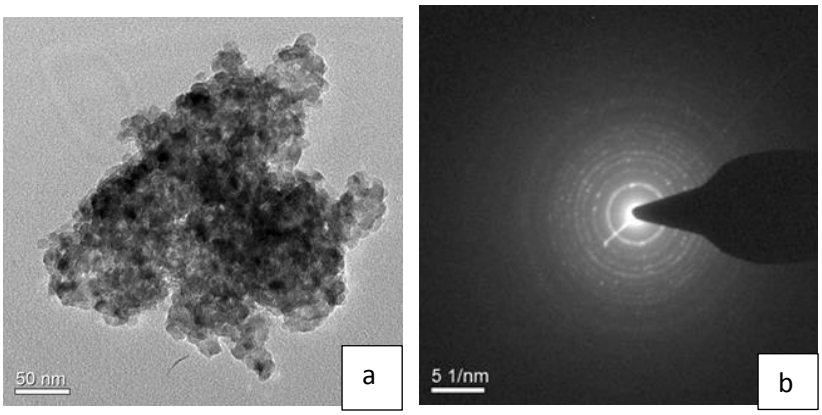

Figure 12. (a) TEM image of biosynthesized TiO_2 (1:1) NPs and (b) its SAED pattern.

Figure 12 (b) illustrates the selected area electron diffraction (SAED) pattern of biosynthesized TiO_2 nanoparticles. Concentric Scherrer's rings are clearly visible, showing orientation in all possible directions, indicating the formation of anatase TiO_2 nanoparticles. The crystalline nature of the biosynthesized TiO_2 nanoparticle was confirmed by the selected area electron diffraction (SAED) pattern with bright circular spots corresponding to (101), (004), (200), (105), (211), (204), (220) and (215), respectively planes of the anatase lattice of biosynthesized TiO_2 nanoparticles. And this SAED pattern shows the polycrystalline nature of the formed nano samples (Figgemeier *et al.*, 2007).

4.5. Ultraviolet-Visible Spectroscopy (UV-Vis) Analysis

The absorption spectra of TiO_2 nanoparticles biosynthesized within 1:1, 2:1 and 1:2 ratios are indicated in Figure 13 (a, b and c), respectively reveals the reduction process and formation of nanoparticles which shows excellent agreement with those reported in the literatures. The band gap energy was determined based on the numerical derivative of the optical absorption coefficient. The fundamental absorption method refers to band to band transitions was obtained by using energy relation: $E_g = \frac{hc}{\lambda}$. From the UV-Vis absorption spectra given in Figure 13 (a), it can be observed that the maximum absorbance of TiO_2 (1:1) NPs was attained at 314 nm and this peak was assigned due to the presence of surface plasmons. Therefore the band gap energy of TiO_2 NPs biosynthesized within a 1:1 ratio was found to be, 3.95 eV. Broadening of the spectrum indicates the polydisplesed of the biosynthesized nanoparticles and the red shift of the absorption curve results in the reduction of the band gap energy and also the recombination rate as compared with that of the UV-Vis spectra of TiO_2 (2:1).

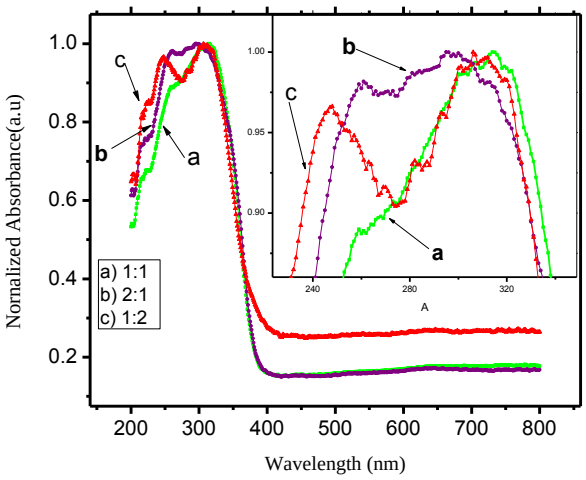

Figure 13. UV-Vis absorption spectra of TiO_2 NPs a (1:1), b (2:1) and c (1:2).

Figure 13 show spectral shift following the difference in ratio. The maximum wavelength for TiO_2 (2:1) was observed at 298 nm. Again the band gap energy of this nanoparticles (2:1) was calculated using the direct band gap method and found to be 4.16 eV. The absorption spectrum of TiO_2 nano samples biosynthesized within 1:1 and 2:1 ratio shows an absorption onset at around 314 and 298 nm, respectivley which is in excellent agreement with the band gap of anatase TiO_2 phase reported previously in the literature (Ashok *et al.*, 2014). The absorption spectra of the biosynthesized TiO_2 (1:2) nanoparticles were also determined. The maximum wavelength was observed at around 306 nm and using this wavelength data it is possible to find the band gap energy and was determined based on the numerical derivative of the optical absorption coefficient /was calculated using direct band gap method. Thus the band gap energy was calculated as 4.05 eV. All the TiO_2 NPs biosynthesized in different ratios exhibit a slight shift of the absorption edge towards the visible region.

4.6. Fourier Transform Infrared (FTIR) Analysis

The FTIR spectrum of biosynthesized titanium oxide nanoparticles showed peaks at 3426.65, 2334.34, 1627.45, 1354.78 and 567.13. From those indicated peaks, the broad absorption peak of titanium dioxide nanoparticles observed at 3426.65 cm^{-1} represents the presence of higher concentration of alcohols, phenols with O-H stretches. The intense peak shown at 2334.34 cm^{-1} indicates the alkene group with C=H stretching. The medium absorption peak indicated at 1627.45 cm^{-1} represents the C=O stretching of primary amide or to C=C groups of aromatic rings. The peak 1627.45 cm^{-1} also reveals bonds of carboxylate group present in the root extract of *k. foliosa* which indicates the binding of proteins with the surface of TiO_2 and thereby it leads to the stabilization of the biosynthesized nanoparticles. The

absorption peak represented at 1627.45 cm^{-1} also indicates the presence of N-H bending mode of vibrations of primary amines. The peaks represented by 1354.78 cm^{-1} shows the aromatic ethers of C-O stretching. This is clearly indicates the presence of biomolecules and bio-constituents from roots of *k. foliosa* extract that leads for the formation of stable TiO_2 NPs. This peak also reveals the presence of C-H alkene rocking structure. In addition to this, the FTIR spectrum of TiO_2 NPs shows diffraction peaks corresponding to the broad band centered at 567.13 cm^{-1} which represents a characteristic peak of Ti-O-Ti bending mode of vibration which confirms the formation of metal oxygen bonding. This peak also indicates that the organic solvent was completely eliminated after the annealing process was completed. This result is consistent with other studies reported by (Vasconcelos *et al.*, 2011). Figure 14 shows the FTIR spectrum of TiO_2 nanoparticles.

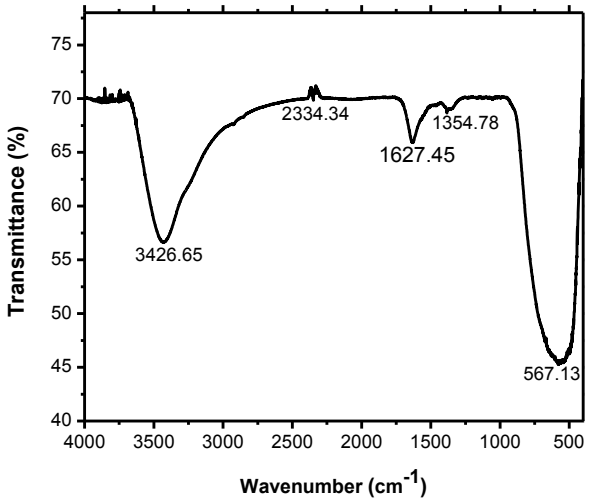

Figure 14. FTIR spectrum of biosynthesized TiO_2 nanoparticles.

Finally, it can be noticed that the presence of different proteins/enzymes, carboxylic acids and amine groups in the root extract of *k. foliosa* can leads to the formation of TiO_2 nanoparticles through stabilization and encapsulation, respectively. Taken as a whole, the FTIR spectrum indicates that the TiO_2 nanoparticles biosynthesized using root extract of *k. foliosa* were surrounded by polyphenols, carbocylic acids, amines, proteins and aromatics ethers. From the FTIR data, it is possible to suggest that the presence of phenolic and amine groups of the extract acts as capping agent on the surface of the TiO_2 nanoparticles and prevent them from aggregation. Thus, we could justify a supportive correlation between the XRD and the FTIR report of the biosynthesized nanoparticles, both confirming the stability and the dispersibility of the nanoparticles.

4.7. Absorption Spectra of Sensitizers

The optical absorption spectra of the prepared ethanolic root extract of *k.schemperi* and a synthetic sensitizer prepared from crystal violet organic dye is shown in Figure 15 and index 3. Natural dye extract of *k.schemperi* and synthetic dye formed from crystal violet using ethanol absolute and distilled water, respectively, were used as photosensitizers during the fabrication of dye sensitized solar cells. The maximum absorbance for this natural sensitizer was 531 nm. The absorption ascribes to the component namely, anthocyanin, a group of natural phenolic compounds (Suganya., 2014). Because anthocyanin shows colors in the range of visible light from red to blue, it is predicted to become highly efficient sensitizer for wide range of semiconductors. This result confirms that the solution of this natural dye can be used as a photosensitizer because their absorption peaks are lying in the UV-Vis region. One of the essential requirements of best performing photosensitizer is broad and intense absorption in the UV-Vis and near-IR region of the solar spectrum (Suganya., 2014). As it can observed from UV-Vis spectra from index 3 dyes extracted from *k.schemperi* absorb photons in the visible portion of electromagnetic radiation. Similarly, the UV-Vis absorption of crystal violet dye in distilled water as a solvent is shown in Figure 15 which exhibits an absorption in the UV-Vis spectrum and it shows a maximum absorbance at around 440 nm.

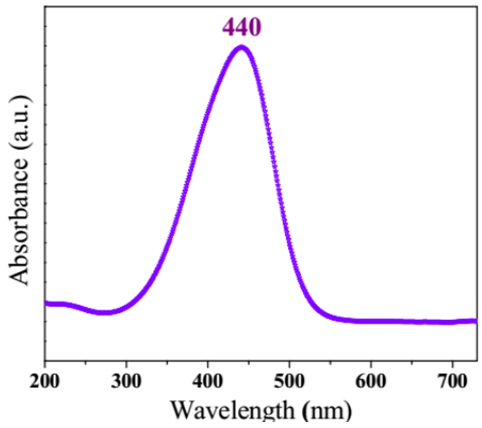

Figure 15. Optical absorption spectra of crystal violet sensitizer.

4.8. Current density Vs Voltage Characteristics of TiO_2 based DSSCs

The photovoltaic tests of the as prepared DSSCs obtained using a natural sensitizer extracted from roots of *k.schemperi* using ethanol absolute as a green solvent and a synthetic sensitizer prepared from crystal violet using distilled water were performed by measuring the current density-voltage (J-V) characteristic curves by using oriel class solar simulator under the standard illumination of light intensity (100 mW/cm^2). The performance of the dyes as sensitizers in DSSCs were evaluated by different parameters

such as J-V (short circuit current density), IPCE (incident Photon to current efficiency also known as quantum efficiency), I_{SC} (short circuit current), V_{OC} (open circuit-voltage), FF (fill-factor). The short circuit-current is the current across the solar cell. The typical current density-voltage (J-V) curves of the as prepared DSSCs using a synthetic organic dye, crystal violet which was prepared using distilled water and a natural dye extracted from roots of *k. schemperi* using absolute ethanol as extracting solvent are shown in Figure 16 and 17, respectively.

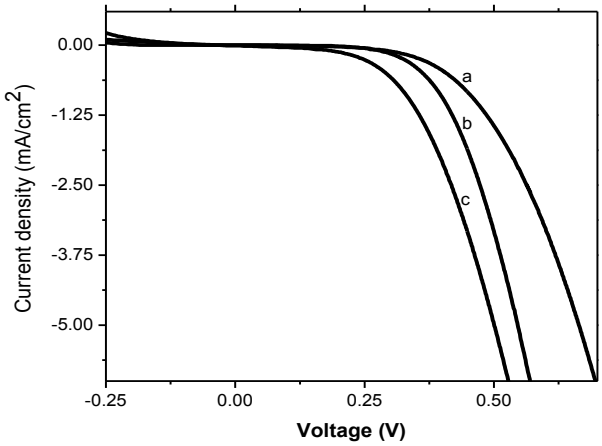

Figure 16. J-V curve of crystal violet based DSSCs using TiO_2 a (1:2), b (1:1) and c (2:1).

As shown from Figure 16 (b) and Table 2, the fill factor (FF) of these DSSCs obtained by using crystal violet sensitizer and TiO_2 (1:1) photoanode shows highest value (79.1%) and also it shows the maximum open circuit voltage. This indicates that PECs based biosynthesized TiO_2 nanoparticles shows relatively well rectification. Which is attributed to better interconnection between the biosynthesized TiO_2 nanoparticle film leading to enhanced electron transport dynamics. Despite TiO_2 (1:1) photoelectrode having lowest efficiency as compared to the remaining two ratios, it was found to have the highest fill factor as it can be observed from Table 2. This has been contributed by the shape of J-V curve of TiO_2 (1:1) in the presence of the sensitizer, which looks better than the rest due to constancy of the current. Therefore, the DSSC constructed using TiO_2 (1:1) have less parasitic losses compared to all the other cells and thus good quality cell. As shown from Figure 16 (c), biosynthesized TiO_2 (2:1) photoanode with the crystal violet sensitizers shows higher short circuit current density and power conversion efficiency than that of the remaining two ratios of the biosynthesized titanium oxide nanoparticles. This is because of the larger the band gap energy of the biosynthesized photoanode. Table 2 shows the performance of biosynthesized TiO_2 nanoparticles based DSSCs using crystal violet sensitizer. As it can be revealed from Table1, the power conversion efficiency of TiO_2 (1:1) is low as compared to the remaining two ratios of the biosynthesized TiO_2 photoelectrode.

Table 2: Photovoltaic performance of biosynthesized TiO_2 based DSSCs using crystal violet dye.

TiO_2 ratio	J_{SC} (mA/cm^2)	V_{OC} (mV)	J_{max} (mA/cm^2)	V_{max} (mV)	P_{max} (mW/cm^2)	FF%	η%
1:1	5.06×10^{-4}	86	9.29×10^{-4}	37	3.44×10^{-2}	79.1	0.034
2:1	8.35×10^{-3}	29	7.4×10^{-3}	18	1.33×10^{-1}	54.9	0.133
1:2	1.29×10^{-3}	49	1.09×10^{-3}	36	3.93×10^{-2}	62.2	0.039

DSSCs constructed with biosynthesized TiO_2 (2:1) photoanode with the presence of crystal violet water prepared sensitizer shows low fill factor (FF = 54.9), this may be due to large series resistance in the cell. Series resistance arises from ohmic resistance, poor connection between materials interface and low mobility of the pepareds electrolyte. As it can be explained in Figure 10 (b), the surface morphology of the biosynthesized nanoparticles possess nearly uniform spherical shape and has larger surface area that enables to absorb sensitizers effectively, then the electron transport cycle is faster and as a result the cell performance/power conversion efficiency is best as compared to the remaining ratios. In water prepared crystal violet sensitizer with TiO_2 (1:1) the short circuit current density is low. This is because of due to the low injection rate of electron into the biosynthesized semiconductor oxide conduction band which inturn decreases the short circuit current density and results in a small power conversion efficiency (Ananth *et al.*, 2014). As it can be revealed in Figure 16 (a) and Table 2, biosynthesized TiO_2 (1:2) photoanode posses the highest open circuit voltage and fill factor next to TiO_2 (1:1) and this inturn reveals that the PEC shows well rectification spectra. Although V_{OC} and FF of DSSC with TiO_2 (2:1) were found to be lower as compared to the other ratios, DSSC with TiO_2 (2:1) was found to have superior conversion efficiency because of its higher short circuit current density (J_{SC}).

As it can be observed from Figure 17 (a, b and c) and table 3, the power conversion efficiency of these DSSCs obtained by using ethanolic root extract of *k.schemperi* sensitizer with TiO_2 (2:1) biosynthesized photoelectrode shows highest value (1.3%) relative to the remaining two ratios and also it shows the maximum open circuit voltage (161 mV).

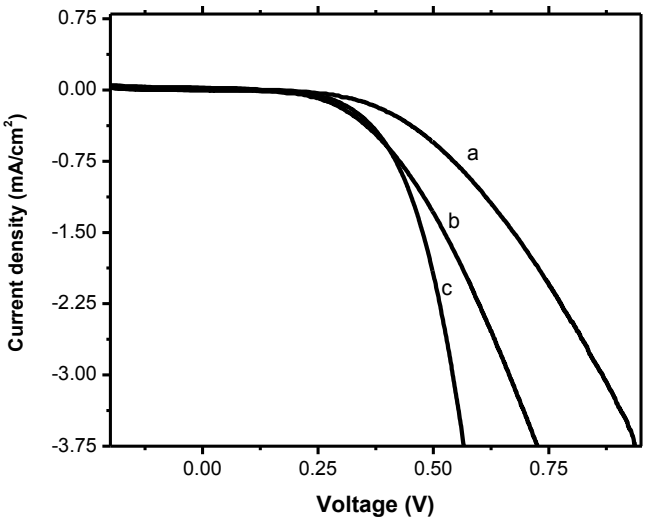

Figure 17. J-V curve of *K.schemperi* based DSSCs using TiO_2 a (2:1), b (1:1) and c (1:2) ratio.

All the devices constructed show low values of incident to photon current conversion efficiency also known as power conversion efficiency (η), this may be due to the fact that, the fast charge recombination rate, loss resulting from the increase traffic of the electron or incompatibility between the energy of the excited state of the adsorbed sensitizers and the conduction band edge of the biosynthesized semiconductor. The improvement in J_{SC} value of TiO_2 (2:1) based DSSC is basically due to the improved absorption of light caused by larger sensitizer coated area of the biosynthesized nanoparticles.

Table 3: Photovoltaic performance of biosynthesized TiO_2 based DSSCs using *k.schemperi* sensitizer.

TiO_2 ratio	J_{SC} (mA/cm^2)	V_{OC} (mV)	J_{max} (mA/cm^2)	V_{max} (mV)	P_{max} (mW/cm^2)	FF %	η%
1:1	$6.05x10^{-3}$	48	$4.17x10^{-3}$	28	$1.17x10^{-1}$	40.3	0.117
2:1	$2.46x10^{-2}$	161	$1.84x10^{-2}$	70.6	1.30	32.8	1.300
1:2	$1.29x10^{-3}$	63	$8.97x10^{-4}$	38	$3.41x10^{-2}$	42	0.034

Accoring to Table 3, the maximum conversion efficiency of DSSCs was observed which was obtanined by using *k.schemperi* ethanolic root extracted with TiO_2 (2:1) photoanode. This is due to the more crystalline nature that allows more dye adsorption and the larger band gap energy of the biosynthesized nanoparticles, higher interaction between TiO_2 (2:1) nano crystalline film and *k.schemperi* ethanolic extract sensitizer which leads to a better charge transfer. In general the efficiencies of DSSCs not only depend on the molecular structure of the natural pigment, but also depends strongly on properties of the biosynthesized photoelectrode such as surface morphology, self assembly and aggregation of the dye molecules (Wasan *et al.*, 2015). This is because due to the surface structure and the surface morphology of biosynthesized nanoparticle based DSSC that enables a strong bonding between the hydroxyl and carboxyl groups present in the natural pigments like anthocyanin with the photoanode resulting in a better performance. As it can be explained in Table 3 in case of TiO_2 (1:2) based DSSCs decrease of J_{SC} may be attributed to slower electron injection of the extracted *k.schemperi* molecules or due to self quenching if they undergo aggregation, either before or during dye adsorption process on the biosynthesized metal oxides and this low value of J_{SC} results low in power conversion efficiency (η). The low power conversion efficiency of natural dye sensitized solar cells are due to the structure of the pigments. In cases where there are interference which hinders for the dye pigments to form bond with the oxide surface of the green synthesized nanoparticles (TiO_2). This will then prevents the molecule from arraying on to the surface of the TiO_2 prepared film effectively (Narayan ., 2012). It has been earlier reported that the conversion efficiency of most of the DSSC made from natural dyes and some organic synthetic dyes suffers from low open circuit voltage which is also the case in the present study where the open circuit obtained ranges from 0.029 - 0.161 V. This can be due to both possible

electron/dye cation recombination pathways and the acidic dye adsorption environment (Narayan., 2012).

4.9. IPCE Characteristics of Biosynthesized TiO_2 based DSSCs

The incident photon to current conversion efficiency (IPCE), defined as the number of electrons generated by light in the external circuit divided by the number of incident photons collected at each wavelength was calculated using equation 5. Photoaction spectra provided further insights on the photoelectrochemical behavior of biosynthesized photoelectrodes with sensitizers. The following Figures (18 and 19) shows the IPCE spectra of TiO_2 (1:1, 2:1 and 1:2) photoelectrodes sensitized with crystal violet dye and ethanolic root extract of *k.schemperi* sensitizer as a function of wavelength. Figure 18 (a, and b) shows the action spectra for the biosynthesized TiO_2 (2:1, and 1:2) based DSSCs sensitized with crystal violet dye. From Figure 18 (a) given in the wavelength range of 300 - 800 nm, the IPCE% plot exhibits relatively a maximum of 18.01% at a wavelength of 360 nm with biosynthesized TiO_2 (2:1) phototelectrode crystal violet sensitized PEC solar cell. This ratio of photoelectrode involves a broad absorption spectra up to 780 nm which covers the wide UV-Vis region. And as a result the IPCE% value is best relative to the other ratio. As it can be shown from Figure 18 (a), the action spectra of TiO_2 (2:1) with crystal violet sensitized PEC solar cells is due to the direct light harvesting by the biosynthesized photoelectrode, TiO_2 (2:1) semiconductor.

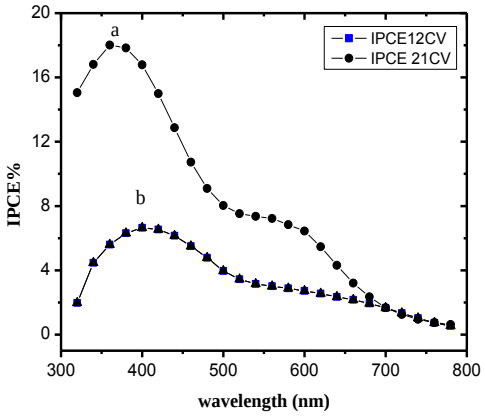

Figure 18. IPCE % Spectra of TiO_2 a (2:1) and b (1:2) based DSSCs using crystal violet dye.

From Figure 18 (b) IPCE% plot exhibits 6.64% at 380 nm with biosynthesized TiO_2 (1:2) in the presence of crystal violet sensitizer. In this case the action spectra originates due to the direct light harvesting by the TiO_2 semiconductor. Relative to TiO_2 (2:1) ratio, TiO_2 (1:2) shows low IPCE% value because of low inefficient light harvesting efficiency. Since the IPCE of DSSC depends on the incident

light harvesting and light scattering properties. Incident light harvesting depends on the surface area of biosynthesized TiO_2 photoelectrode and the dye adsorbed amount where as light scattering phenomenon depends on the surface morphology and surface structure of the TiO_2 photoelectrode. This low LHE can be made due to low dye absorption coefficient over the solar spectrum, a thin TiO_2 film to support large concentration of adsorbed crystal violet which absorbs a significant fraction of the incident light, insufficient light scattering within the prepared TiO_2 (1:2) film. Again this low IPCE% value may also arise due to the average distance that the electrons travel. The electron collection efficiency is an indication of the probability that a photogenerated electron reaches the collecting substrate contact before it is lost by electron dye-recombination (Halme *et al.*, 2010). The collection efficiency thus depends on the average distance that electrons travel before recombination. As it can be observed from the J-V spectra and IPCE% spectra, the results from the IPCE% data are found to be consistent with the results from the J-V curves already obtained, i.e maximum DSSCs efficiency and maximum IPCE% value in both cases is obtained using biosynthesized TiO_2 (2:1) photoanode.

As it can be observed in Figure 19 (a), from the photoaction spectra, relatively maximum IPCE% value was obtained using TiO_2 (2:1) in the presence of ethanolic root extract of *k.schemperi* sensitizer and this value is 8.11% which was located at a wavelength of 340 nm. The improvement of IPCE% for this biosynthesized photoelectrode results from higher electron transportation at the electrolyte interfaces and good electrocalytic activity of the photoelectrode (*Ò*Regan *et al.*, 2005). As it can be explained from SEM image at Figure 10 (b), the biosynthesized nanoscale roughness and spherical like surface morphology provide large surface area for adsorption of the dye and high electrocatalytic activity. Again TiO_2 (1:1) with the presence of *k.schemperi* sensitizer posses an IPCE% of 2.66% which occurs at 500 nm. This action spectra response is contributed by sensitization of roots of *k.schemperi* ethanolic extracts.

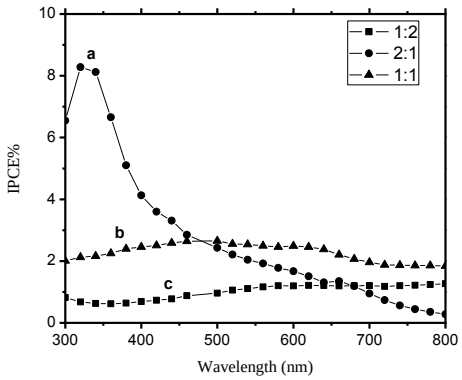

Figure 19. IPCE% spectra of TiO_2 a (2:1), b (1:1) and c (1:2) based DSSCs using *kniphofia schemperi*.

As it can be shown from Figure 19 (c), low IPCE% value was recorded using biosynthesized photoelectrode obtained within a 1:2 ratio in the presence of ethanolic root extract of *k.schemperi* and this value was calculated as 1.27% at 800 nm. This low value of IPCE% may be attributed by inefficient light harvesting efficiency (LHE) by the dye that is inefficient charge injection into the prepared TiO_2 film, or inefficient collection of injected electrons. The results from the IPCE% data were found to be consistent with the results from the J-V curves already obatined. Generally all the fabricated devices show low value of IPCE%. This may be because of most of the sensitizers may be attached with the biosynthesized film of the nanoparticles by means of weak physical attaching or by a weak bonding.

5. CONCLUSION AND RECOMMENDATION

5.1. Conclusion

Biosynthesis of titanium oxide nanoparticles using *k.foliosa* root extract has been demonstrated. TiO_2 NPs were successfully biosynthesized using titanium tetra butoxide precursor and *k.foliosa* ethanolic root extract within different ratios and the biosynthesized NPs were characterized by advanced istruments. Biosynthesis of TiO_2 NPs was found to be plant extract dependent i.e good result was obtained when it is biosynthesized within a 1:1 ratio and when the ratio of the precursor used is much greater, when the plant extract used is greater than the amount of the precursor used, the crystalline nature is lost because it is beyond the coating surface and matrix of TiO_2. Thermal analysis revealed that the biosynthesized TiO_2 was stable above 500 ℃. XRD result indicates that the particles size was found to be from 8.17- 10.15 nm. SEM analaysis result indicates spherical shape of the formed nano samples. EDX analysis shows the presence of only Ti and O and absence of foreign matter indicates the purity of the formed nano samples. TEM analysis reveals that the internal structure of the biosynthesized NPs were spherical shape and posses good crystalline nature in its SAED pattern as supported by SEM and XRD. UV-Vis result shows an absorption from 298 - 314 nm. FTIR analysis indicates the presence of various capping agents in the root extract of *k.foliosa*. Root of *k.schemperi* was used as a natural sensitizer which was obtained using absolute ethanol as a solvent and crystal violet was used as organic synthetic dye. In this study the photovoltaic parameters of the biosynthesized TiO_2 NPs in different ratios with the presence of root extract of *k.schemperi* and crystal violet dye was demonstrated. The highest short circuit current obtained was 0.0246 mA/cm^2 and open circuit voltage of 161 mV which was achieved using TiO_2 (2:1) photoelectrode. The biosynthesized TiO_2 (1:1) NPs shows relatively a maximum fill factor value of 79.1%. Relative to the remaining two ratios of TiO_2 NPs, maximum power conversion efficiency of 1.3% was achieved using TiO_2 (2:1) photoelectrode. The biosynthesized photoelectrode shows an IPCE% of 18.01%, 6.64% and 2.66% using TiO_2 (2:1, 1:2 and 1:1) ratios.

5.2. Recommendation

The area explored several important informations towards the biosynthesis of TiO_2 nanoparticles using environmentally friendly, low cost, easily achiviable method and its applicatios for DSSCs. As a result the following future recommendations can be made for further researches based on the findings of the present study.

To predict the right reaction mechanism between organic compounds obtained from the plants used during synthesis processs with that of the precursor solution, characterization of biomolecules obtained from the plant using NMR spectroscopy provides the exact molecular structure of the compound obtained from the plants already used. This characterization method allows to know the chemical structure of the compound and its functional groups. Then, it is possible to know what type of compounds are present and used as a reducing and capping agent. Therefore, the biomolecules used as a reducing and capping agent in the biosynthesis of NPs will be characterized using NMR spectroscopy.

Brunauer Emmett teller (BET) surface area analysis of each ratio of the biosynthesized TiO_2 NPs allows to select the best photoanode that posses high surface area which provides to select best photoanodes that allows large dye adsorption.

Analysis of the functional groups of the natural sensitizers used in DSSCs provides the presence of various functional groups and it will allow to select the best sensitizer that possesses double bond conjugated species and consequently the cell performance could be improved. Therefore, the structure of the sentisizer will be done using FTIR spectroscopy before socking in to the corresponding solvent.

REFERENCE

ÓRegan. B, Grätzel. M., (1991). A low-cost, high-efficiency solar cell based on dye-sensitized colloidal TiO_2 films. *Nat*, 353 : 737-740.

ÒRegan. B. C, Scully. S, Mayer. A. C, Palomares. E, Durrant. J., (2005). An efficient and low-cost TiO_2 compact layer for performance improvement of dye-sensitized solar cells. *J Phys Chem.* B., 109 : 4616.

Abate. G, and Etse. D, Demissew. S., (1989). Ethiopian Traditional Medicin. Addis Ababa University Press. Addis Ababa, 99 -183.

Al-Alwani. M. A. M, Mohamad. A. B, Kadhum. A.A.H and Ludin. N. A., (2015). Natural dye extracted from Pandannus amaryllifolius leaves as sensitizer in fabrication of dye-sensitized solar cells. *Mol Biomol Spectrosc. Acta Part* A, 138 : 130.

Ananth. S, Arumanayagam. T, Vivek. P, Murugakoothan. P., (2014). Natural dye extracted from Pandannus amaryllifolius leaves as sensitizer in fabrication of dye-sensitized solar cells. *Optiks Int J Light Ele Optics*, 125 : 495.

Archana Maurya, Pratima Chauhan, Amita Mishra, and Abhay. K. Pandey, (2012). Surface functionalization of TiO_2 with plant extracts and their combined antimicrobial activities against E. Faecalis and E. Coli. *J. Res. Updates Poly. Sci.*, 1: 43 - 51.

Ashok. CH, Venkateswara. Rao. K., (2014). ZnO/TiO_2 nanocomposite rods synthesized by microwave-assisted method for humidity sensor application. *Superlattice Microst.*, 76 : 46.

Baker. S, D. Rakshith, Kavitha. K. S, Santosh. P, Kavitha. H.U, Rao. Y, atish. S. S., (2013). Plants emerging as nanoparticles towards facile route in synthesis of nanoparticles. *Biol Impacts*, 3: 111.

Brayner. R., (2008). The toxicological impact of nanoparticles. *Nano today*, 3: 48.

Calogero. G, Dimarco. G, Cazzanti. S, Caramori. S, Argazzi. R, Dicarlo. A, Bignozzi. C.A., (2010). Dye Sensitized Solar Cells Using Natural Pigments from Five Plants and quasi-solid State Electrolyte. *Int J Mol Sci.*, 11: 254.

Carp. O, Huisman. C. L, Reller. A., (2004). Photoinduced Reactivity of Titanium dioxide. *Prog Solid State Chem.*, 32(2): 33 - 177.

Chanathaworn. J, Bunyakan. C, Wiyaratn. W., Chungsiriporn. J., (2012). Photocatalytic decolorization of basic dye by TiO_2 nanoparticle in photoreactor. Sonklanakarin: *J Sci Tech.*, 34: 203.

Chang Kook Hong, (2015). Electrochemical Properties of Electrodeposited PEDOT Counter Electrode for DSSC. *Int J Electrochem Sci.*, 10: 5521 - 5529.

Chang. H, Wu. HM, Chen. TL, Huang. KD, Jwo. CS, Lo. YJ., (2010). Dye-sensitized solar cell using natural dyes extracted from spinach and ipomoea. *J Alloy Compd.*, 495 : 606-10.

Chappel. S, Ofir. L. G, A, Zaban., (2005). Extending the current Collector into the Nanoporous Matrix of Dye Sensitized Electrodes. *J Phy Chem* B., 109 : 1643-1647.

Dagne. E, Steglich. W., (1984). Knipholone: a unique anthraquinone derivative from *Kniphofia foliosa*. *Phytochem.*, 23: 1729 - 1731.

Dahlgren. R. M.T, Clifford, H.T, Yeo, P.F., (1985). The Families of the Monocotyledons. Springer-Verlag, Berlin.

Emery. K., (2015). Progress in Photovoltaics Research and Applications. *NREL*., 23(1): 1 - 9.

Fan. L, Kang. S, Wu. J, Hao. S, Lan. Z, Lin. J., (2010). "Quasi-solid state Dye-sensitized solar cells based on polyvinylpyrrolidone with ionic liquid". *J* Energy sourc A., 32 : 1559.

Fan-Tai Kong, Song-Yuan Dai, Kong-Jia Wang, (2017). Review of Recent Progress in Dye-Sensitized Solar Cells. A *Rev Art.*, 2007: 75384.

Figgemeier. E, Kylberg.W, Constable. E, M. Scarisoreanu, Alexandrescu. R, Morjan. I Soare. I, Birjega. R, Popovici. E, Fleaca. C, Gavrila-Florescu. L, Prodan. G., (2007). Titanium dioxide nanoparticles prepared by laser pyrolysis: Synthesis and photocatalytic properties. *Appl Surf Sci.*, 254 : 1037-1041.

Gao.Y, Masuda.Y, Peng. Z, Yonazawa. T, Kaumoto. K., (2007). Green synthesis of TiO_2 and its Photocatalytic activity. *J Mater Chem.*, 13 : 608.

Gong. J, Liang .J, Sumathy. K, (2012). Review on dye-sensitized solar cells, Energy Reviews. *Inorg Chem*., 16: 5848 - 5860

Grätzel. M, Janssen. R. A. J, Mitzi. D. B, Sargent. E. H., (2012). Materials interface engineering for solution-processed photovoltaics. *Nat.*, 488: 304 - 312.

Grätzel. M, (2004). Structurally stabilized mesoporous TiO_2 nanofibres for efficient dye-sensitized solar cells. *J Photochem Photobiol.,* A 164 : 3 - 14.

Hafez. H, Lan. Z, Liwu. Q., (2010). High efficiency dye-sensitized solar cell based on novel TiO_2 nanorod/nanoparticle bilayer electrode. *J Nanotech Appl Sci.,* 3: 45 - 50.

Hagfeldt .A, Gr*ä*tzel. M., (1995). Light induced redox reactions in nanocrystalline systems. *Chem. Rev.,* 95: 49 - 68.

Halme. J, Vahermaa. P, Miettunen. K, Lund. P., (2010). Natural dye sensitized phothoelectrochemical cells based on zinc oxide nanoparticles. *Adv Mater.*, 22 : 210-221.

Hamann. T.W, Ondersma. J.W., (2011). Dye-sensitized solar cell redox shuttles. *Energy Environ Sci.*, 4(2): 370 - 381.

Hao. S, Wu. J, Huang. Y, Lin. J.,(2006). Natural dyes as photosensitizers for dye-sensitized solar cell. *Sol Energy*, 80 : 209-14.

Hedbor. S, Klar. L., (2005). Plant extract sensitized nanoporous TiO_2 thin film photoelectrochemical cells, Master thesis, Uppsala.

Hoffmann. M. R, Martin. M.T, Choi. W, Bahnemann. D.W., (1995). Environmental applications of semiconductor photocatalysis. *Chem Rev.*, 95: 69 - 96

Huang. H, Zhao. H, Cao. Z, Li. X, Zhang. L, Liu. X., (2012). Completely transparent conducting oxide free and flexible dye-sensitized solar cells fabricated on plastic substrates. *Inorg Chem.*, 162: 231.

Hudlikar. M, Joglekar S, Dhaygude M., Kodam K., (2012). Green synthesis of TiO_2 nanoparticles by using aqueous extract of *jatropha curcas* L. latex. *Mater Lett.,* 75: 196 -199.

Jasim. K. E., (2011). DSSCs working principle, challenging and opportunities. *Int J* NPs., 12: 172.

Jose. R, Thavasi.V, Ramakrishna. S., (2009). Metal oxides for dyesensitized solar cells. *J Am Soc.*, 92: 289 - 301.

Kang. S. H, Choi. S. H, Kang. M. S, Kim. J.Y, Kim. H. S, Hyeon.T, Sung. Y.E., (2008). Nanorod Based Dye-Sensitized Solar Cells with Improved Charge Collection Efficiency. *Adv Mater.,* 20: 54 - 58.

Kayama.Y, Miki. T, Wang, X. F, Nagae, H., (2009). plant flower pigment sensitized photoelectrochemical cell based nanostructured TiO_2. *Int J Mol Sci.,* 10 : pp. 4575.

Koumura. N, Zhong-sheng Wang, Mori. S, Miyashita. M, Suzuki. E, Hara. K., (2006). Alkyl-functionalized organic dyes for efficient molecular photovoltaics. *J Am Chem Soc.*, 128 (44) : 14256 -14257.

Kumar T, Rahuman A. A, Jayaseelan C, Rajakumar G, Marimuthu S, Kirthi V.A, Velayutham K, Thomas J, Venkatesan, Kim K-S., (2014). Green synthesis of titanium dioxide nanoparticles using *psidium guajava* extract and its antibacterial and antioxidant properties. *Asian Pac J Trop Dis.,* 968-976.

Kusama. H., Arakawa. H., (2005). Progress on the electrolytes for dye-sensitized solar cells. *Sol Energy Mater Sol Cells*, 85: 333.

Liao. J.Y., Lei . X. B., Kuang. B. D., Su. Y. C., (2011). Tri-functional hierarchical TiO_2 spheres consisting of anatase nanorods and nanoparticles for high efficiency dye-sensitized solar cells. *Energy Environ Sci.,* 4 : 4079 - 4085.

Loo. Y.Y, Chieng. B.W, Nishibuchi. M, Radu. S., (2012). Synthesis of nanoparticles by using tea leaf extract from Camellia sinensis. Int J Nanomed., 7: 42 - 63.

Macht. B, M, Turrion. A, Barkschat. P, Salvador. K, Ellmer, Tributsch. H., (2002). Effects of water intrusion on the charge-carrier dynamics, performance, and stability of dye sensitized solar cells. *Sol Energy Mater Sol Cells*, 73: 163 - 173.

Malarkodi. C, Chitra. K, Rajeshkumar. S, Gnanajobitha. G, Paulkumar. K, Vanaja. M, Annadurai. G., (2013). Novel eco-friendly synthesis of titanium oxide nanoparticles by using Planomicrobium sp. and its antimicrobial evaluation, *Der Pharmacia Sinica,* 4(3): 59-66.

Mandal. D, Bolander. M, Mukhopadhyay. E, Sarkar. D , Mukherjee. G, (2006). The use of microorganisms for the formation of metal nanoparticles and their application. *Appl Microbiol Biotechnol.*, 69: 485.

Marimuthu. S, Rahuman. A. A, Jayaseelan. C, Kirthi. V. A, Santoshkumar. T, Velayutham. K, Bagavan. A, Kamraj C, Elango G, Iyappan. M, Siva. C, Karthik. L, Rao. B.V.K., (2013). Acaricidal activity of synthesized titanium dioxide nanoparticles using *calotropis gigantea* against rhipicephalus microplus and haemaphysalis bispinos. *Asian Pac J Trop Dis.,* 682- 688.

Mbonyiryivuze. A, Omollo. I, Ngom. B. D, Mwakikunga. B, Dhlamini. S. M, Park. E, Maaza. M, (2015). "Natural dye sensitizer for Grätzel cells: Sepia melanin." *Phys Mater Chem.*, 3: 1 - 6.

Miettunen. K. K, Halme. J, Saukkonen.T, M. Toivola, Lund. M. P. D., (2009). Performance degradation of dye sensitized solar cells on flexible stainless steel substrates Proc. of the 24th Europen photovoltaic solar energy Conference. Hamburg, Germany, 21 - 25 September.

Mosurkal. R, He. J, Yang. K, Samuelson. L. A, Kumar. J., (2004). Organic Photosensitizers With Catechol Groups for Dye-Sensitized Solar Photovoltaic. *J Photochem Photobiol.*, 168 : 191-196.

Mounir Alhamed, Ahmad. S, Issa. A, Wael Doubal, (2012)." Studying of Natural Dyes Properties as Photo-sensitizer for DSSC". *J. Electron Devices*, 16: 1370 -1383.

Mulati. D. M, Timonah. N. S, Bjorn.W., (2012). The absorption spectra of natural dyes and their suitability as a sensitizer in organic solar cell. *Organic Sol Cells*, 14 (1) : 45 - 60.

Muneer M. Ba-Abbad, Abdul Amir H. Kadhum, Abu Bakar Mohamad, Mohd S. Takriff and Kamaruzzaman Sopian, (2012). Synthesis and Catalytic Activity of TiO_2 Nanoparticles for Photochemical Oxidation of Concentrated Chlorophenols under Direct Solar Radiation. *Int J Electrochem Sci.*, 7: 4871.

Murphy.S. B. R., (1998). In Polymer Networks Principles of their formation, Structure and Properties, R. F. T. Stepto (Ed.), Blackie Academic, London.

Narayan J.K. 2012. Review: Dye Sensitized Solar Cells Based on Natural Photosensitizers. Renew Sust Energ Rev., 16: 208 - 215

Nazeeruddin. M. K, Kay. A, Rodicio. I, Humphrey-Baker. R, Muller. E, Liska. P, Vlachopoulos. N, Gratzel. M.,(1993). Dye Sensitized Solar Cells Using Natural Pigments from Five Plants and Quasi-Solid State Electrolyte. *J Am Chem Soci.*, 115 : 6382.

Nazeeruddin. M. K, Rodicio. K, Humphry-Baker. I, Muller. R, liska. E, Volachopouloes. P., (1993). Conversion of light to electricity by cis-X_2 bis (2, 20 -bipyridyl-4,40 - dicarboxylate) ruthenium (II) charge-transfer sensitizers (X¼Cl , Br , I ,CN and SCN) on nanocrystalline titanium dioxide electrodes. *J Am Chem Soci*, 115 (14) : 6382 - 6390.

Nithya. A, Rokesh. K, Jothivenkata chalam K., (2013). Biosynthesis, characterization and application of titanium dioxide nanoparticles. *Nano vision*, 3(3): 169 - 174.

Prabu1. K. M, Anbarasan. P. M., (2014). Improved performance of natural dye-sensitized solar cells using ZnO doped TiO_2 nanoparticles by sol-gel method. *Int J Sci Res.,*, 3(6) : 2319 - 7064.

Pusit Pookmanee, Sukon Phanichphant, (2009). "Titanium dioxide powder prepared by a sol-gel method." *J Ceram Process Res.*,10(2) : 167- 170.

Rajakumar. G, Rahuman A. A, Priyamvada. B, Khanna V.G., Kumar D. K, Sujin P. J., (2012). Eclipta prostrate leaf aqueous extract mediated synthesis of titanium dioxide nanoparticles. *Mater Lett.*, 68: pp. 115-117.

Ramimoghadam. D, Bagheri. S, Hamid A. S. B., (2014). Biotemplated synthesis of anatase titanium dioxide nanoparticles via lingo cellulosic waste material. *Biomed Res Int.*, 205636 : 1-7.

Ramimoghadam. D. M. Z, Bin Hussein, Y. H. Taufiq-Yap,(2013). "Hydrothermal synthesis of zinc oxide nanoparticles using rice as soft biotemplate." *Chem Cent J.*, 7(1) : 36.

Rao. G. K, Ashok. C, Rao V. K, Chakra. S.C, Rajendar. V., (2015). Synthesis of TiO_2 nanoparticles from orange fruit waste. *Int J Multi Adva Res Trend*, 2(1): 82- 90.

Realpe. A, Salamanca. A, Acevedo. M., (20150. Effect of electrolyte type on the hydrogen production using a plate electrolyzer. *Int J Appl Engi.*, 10(9): 23871-23880.

Reza Hemmatzadeh, Ahmad Mohammadi, (2013). Improving optical absorptivity of natural dyes for fabrication of efficient dye-sensitized solar cells. *J Theoretical Appl Phys.*, 7 (57) : 17 - 44.

Rodriguez-Sanchez. L, Blanco. M. C., and Lopez-Quintela M. A., (2000). "Electrochemical synthesis of silver nanoparticles." *J Phys Chem.*, 104(41): 9683 - 9688.

Sankar. R, Rizwana. K, Shivashangari. K. S and Ravikumar. V., (2015). Ultra rapid photocatalytic activity of Azadirachta indica engineered colloidal titanium dioxide nanoparticles. *Appl Nanosci.*, 5: 731- 736.

Santhosh kumar.T, Rahuman. A, Jayaseelan. C, Rajakumar. G, Marimuthu. S, Kirthi. A., (2014). Green synthesis of titanium dioxide nanoparticles using Psidium guajava extract and its antibacterial and antioxidant properties. *Asian Pac J Trop Dis.*, 7 : 968 -76.

Shi. D, Pootrakulchote. N, Guo. R. Li, J., Wang. J.Y, Zakeeruddin. S.M, Grätzel. M, Wang. W., (2008). Empirical Polarity Parameters for Hexaalkylguanidinium-based room-temperature Ionic Liquids. *J Phys Chem.*, C, 112: 17046 - 17050.

Shilpa Hiremath, Mukunthan. K and Balaji .S., (2012). Cashew apple juice (Anacardium occidentale L.) speeds upthe synthesis of silver nanoparticles. *Int J Green Nanotechnol Biomed.,* 4: 71 - 90.

Sisay. T., (2012). Bulk heterojunction, Natural, and Synthetic Dye sensitized Photoelectrochemical solar energy conversion, PhD thesis, Addis Ababa University.

Suganya. P., (2014). The effects of temperature and pH on stability of anthocyanins from red sorghum (Sorghum bicolor) bran. *Afr J Food Sci.,* 6 (24) : 567-573.

Takele. A. L , G.G. Gonfa, Anshebo.T.Y., (2014). Dye-sensitized solar cell using extract of *Jacaranda mimosifolia* and *Salvia spelendens* as a natural sensitizer. *Chem Mater Res.,* 6 (12): 126 - 133**.**

Tamasa panigrahi, Dr. suman jha, (2013).“synthesis and characterization of silver nanoparticles using the leaf of *Azadirachtaindica*”. *J Radiat Res Appl Sci., 1* : 12.

Tarasevich. M. R, Khrushcheva. E. I, Conway. in: B.E, Bockris. J.O’M, White (Eds.). R.E., (1989). *Modern Aspects of Electrochemistry*, Plenum Press, New York, 19 : 295.

Vahermaa. J. P, Miettunen. K, Lund. P., (2010). Interface electric properties of Si/organic hybrid solar cells using impedance spectroscopy analysis. *Adv Mater.*, 22 : 210 - 221.

Vasconcelos D. C. L, Costa V.C, ENunes H. M, Sabioni A. C. S, Gasparon. M, VasconcelosW. L, (2011). Infrared Spectroscopy of Titania Sol-Gel Coatings on 316L Stainless Steel. *Mat Sci Appl.,* 2 : 1375-1382.

Velayutham. K, Rahuman. A. A, Rajakumar. G, Santhoshkumar. T, Marimuthu. S, Jayaseelan. C,.(2012). Evaluation of *Catharanthus roseus* leaf extract mediated biosynthesis of titanium dioxide nanoparticles against Hippobosca maculata and Bovicola ovis. *Parasitol Res.,* 111(6) : 2329-2337.

Vijayalakshmi. R, Rajendran.V., (2012). “Synthesis and characterization of nano-TiO_2 via different methods.” *Archi Appl Sci Res.,* 4(2) : 1183 - 1190.

Vijaylaxmee, Mishra, Richa Sharma, Nakuleshawar, Dut Jasuja and Deepak Kumar Gupta, (2014). “A Review on Green Synthesis of Nanoparticles and Evaluation of Antimicrobial Activity.” *Int J Green and Herbal Chem,* 3(1) : 81 - 94.

Vlachopoulos. N, Liska. P, Augustynski. J, Gr*ä*tzel. M., (1988). Very efficient visible light energy harvesting and conversion by spectral sensitization of high surface area polycrystalline titanium dioxide films *J Am Chem Soc.*, 110: 1216 - 1220.

Wang. Z.S, Sayama. K, Sugihara. H., (2005). Liquid Redox Electrolytes for Dye-Sensitized Solar Cells. *J Phys Chem* B., 109: 22449 - 22455.

Wasan Maiaugree (2015). A dye sensitized solar cell using natural counter electrode and natural dye derived from mango steen peel waste. *Sci Rep.,* 5 : 15230

Whitehouse, C. (2002). Asphodelaceae: flora of tropical East Africa, Beentje, H.J.A. ed. Balkema Publishers Rotterdam, 1-19.

Xu. J, Li. L, Yan. Y, Wang. H, Wang. X, Fu. X, Li. G., (2008). Synthesis and photoluminescence of well dispersible anatase TiO_2 nanoparticles. *J Colloid and interface Sci.,* 318 : 29 - 34.

INDEX

Index 1: SEM images of selected area for EDS spectrum analysis of biosynthesized TiO_2 (1:1).

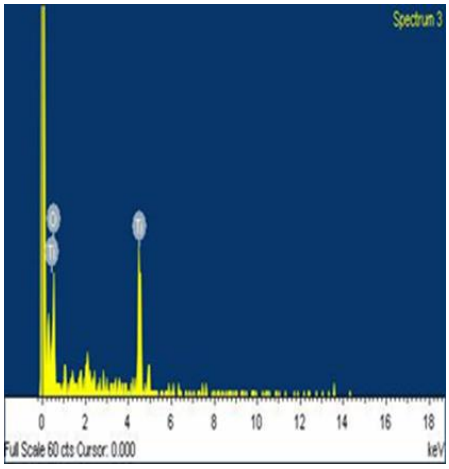

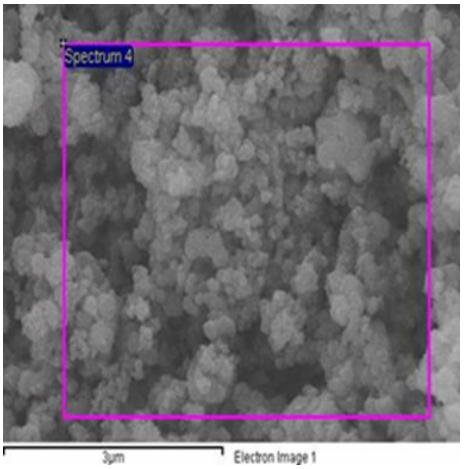

Element	Wt%	At%
Ok	54.81	78.41
Tik	45.19	21.59
Total	100.00	

Index 2: SEM images of selected area for EDS spectrum analysis of biosynthesized TiO_2 (1:2).

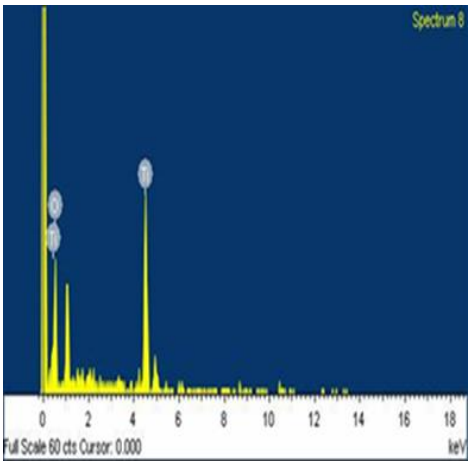

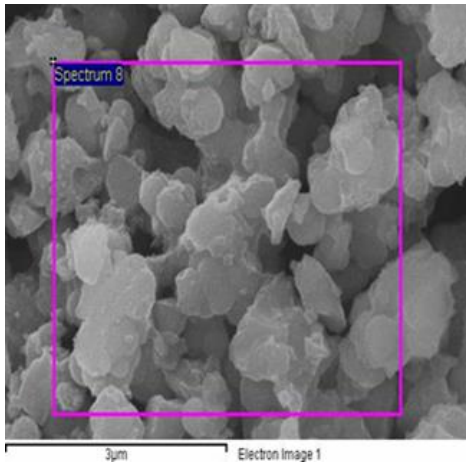

Element	Wt%	At%
Ok	57.95	80.49
Tik	42.05	19.51
Total	100.00	

Index 3: UV-Vis absorption spectra of *kniphofia schemperi* ethanolic root extract sensitizer.